Published July 11, 2016

Different cAMP sources are critically involved in G protein–coupled receptor CRHR1 signaling

Carolina Inda,[1,2] Paula A. dos Santos Claro,[1,2] Juan J. Bonfiglio,[1,2] Sergio A. Senin,[1] Giuseppina Maccarrone,[3] Christoph W. Turck,[3] and Susana Silberstein[1,2]

[1]Instituto de Investigación en Biomedicina de Buenos Aires-CONICET-Partner Institute of the Max Planck Society, C1425FQD Buenos Aires, Argentina
[2]Departamento de Fisiología, Biología Molecular y Celular, Facultad de Ciencias Exactas y Naturales, Universidad de Buenos Aires, C1428EHA Buenos Aires, Argentina
[3]Department of Translational Research in Psychiatry, Max Planck Institute of Psychiatry, 80804 Munich, Germany

Corticotropin-releasing hormone receptor 1 (CRHR1) activates G protein–dependent and internalization-dependent signaling mechanisms. Here, we report that the cyclic AMP (cAMP) response of CRHR1 in physiologically relevant scenarios engages separate cAMP sources, involving the atypical soluble adenylyl cyclase (sAC) in addition to transmembrane adenylyl cyclases (tmACs). cAMP produced by tmACs and sAC is required for the acute phase of extracellular signal regulated kinase 1/2 activation triggered by CRH-stimulated CRHR1, but only sAC activity is essential for the sustained internalization-dependent phase. Thus, different cAMP sources are involved in different signaling mechanisms. Examination of the cAMP response revealed that CRH-activated CRHR1 generates cAMP after endocytosis. Characterizing CRHR1 signaling uncovered a specific link between CRH-activated CRHR1, sAC, and endosome-based signaling. We provide evidence of sAC being involved in an endocytosis-dependent cAMP response, strengthening the emerging model of GPCR signaling in which the cAMP response does not occur exclusively at the plasma membrane and introducing the notion of sAC as an alternative source of cAMP.

Introduction

G protein–coupled receptors (GPCRs) are the largest family of membrane proteins and mediate most cellular responses to neurotransmitters, peptide hormones, lipids, and sensory stimuli, as well as therapeutic drugs. The classical role of GPCRs is to couple the binding of ligands to the activation of specific heterotrimeric G proteins, leading to the regulation of downstream effector proteins. Signaling responses are attenuated by desensitization via a series of steps that uncouple GPCR from G proteins and lead to receptor internalization/down-regulation. However, this traditional view has been replaced by a much more complex signaling model. G protein–independent mechanisms and, more recently, signaling from endosomal compartments have been described for several GPCRs (Rajagopal et al., 2010; Lohse and Calebiro, 2013; Vilardaga et al., 2014).

Corticotropin-releasing hormone (CRH) is a 41-aa peptide that plays a critical role in the integration of neuroendocrine, autonomic, and behavioral responses to stress. Hypothalamic CRH-secreting neurons drive both basal and stress-induced activation of the hypothalamic-pituitary-adrenal (HPA) axis. In addition, CRH is widely distributed in the brain, where it functions as a neuromodulator, integrating a complex system that regulates several aspects of the behavioral stress response. Dysregulation of CRH action through its high-affinity type 1 receptor (CRHR1) is crucial in the pathogenesis of affective disorders (Holsboer and Ising, 2010).

CRHR1 is a class B/secretin-like GPCR that, upon ligand activation, signals mainly by Gs coupling, leading to cyclic AMP (cAMP) increase and activation of multiple signaling cascades (Bonfiglio et al., 2011). In particular, CRH-stimulated CRHR1 signals through extracellular signal regulated kinase 1/2 (ERK1/2) to induce proopiomelanocortin (*Pomc*) transcription and activate the HPA axis in pituitary corticotrophs and in specific brain structures related to behavioral aspects of stress in response to intracerebroventricular CRH administration (Refojo et al., 2005). We have previously described that in a hippocampal neuronal context, CRHR1-mediated ERK1/2 activation triggered by CRH is biphasic, with an early phase peaking at 3–6 min that is dependent on B-Raf and protein kinase A (PKA) and a late phase of sustained ERK1/2 phosphorylation (20–60 min) dependent on CRHR1 internalization and β-arrestin2 (Bonfiglio et al., 2013).

Correspondence to Susana Silberstein: ssilberstein@ibioba-mpsp-conicet.gov.ar

J.J. Bonfiglio's present address is Max Planck Institute for Biology of Ageing, 50931 Cologne, Germany.

Abbreviations used in this paper: 2-HE, 2-hydroxyestradiol; CRH, corticotropin-releasing hormone; CRHR1, CRH receptor 1; ddA, 2′,5′-dideoxyadenosine; ERK1/2, extracellular signal regulated kinase 1/2; FRET, Förster resonance energy transfer; GPCR, G protein–coupled receptor; HPA, hypothalamic-pituitary-adrenal; PKA, protein kinase A; sAC, soluble adenylyl cyclase; tmAC, transmembrane adenylyl cyclase.

The Rockefeller University Press $30.00
J. Cell Biol.
www.jcb.org/cgi/doi/10.1083/jcb.201512075

Published July 11, 2016

The ubiquitous second messenger cAMP regulates numerous, often concurrent, cellular processes. Its activity is tightly regulated and localized to discrete microdomains within the cell to ensure precise spatiotemporal signaling. GPCR-mediated cAMP production was initially thought to depend exclusively on activation of transmembrane adenylyl cyclases (tmACs) at the plasma membrane. More recently, a wealth of research has shown that some activated GPCRs continue to signal by cAMP generation after internalization, thereby defining endocytic cAMP microdomains (Vilardaga et al., 2014). There are nine G protein–regulated tmACs that have different regulatory properties (Willoughby and Cooper, 2007). Furthermore, a second source of cAMP exists in mammalian cells. Soluble adenylyl cyclase (sAC) is an evolutionarily conserved enzyme that is insensitive to G protein regulation but is directly activated by bicarbonate (Chen et al., 2000) and calcium ions (Jaiswal and Conti, 2003; Litvin et al., 2003). sAC is localized throughout the cell, enabling the production of cAMP in different intracellular locations close to specific cAMP targets (Zippin et al., 2004; Tresguerres et al., 2011; Lefkimmiatis et al., 2013).

Combining molecular and pharmacologic tools with Förster resonance energy transfer (FRET)–based biosensor technology, we show that the CRHR1-triggered cAMP response does not exclusively depend on tmACs but also involves sAC as a second source of cAMP. Both cAMP sources play a role in the early ERK1/2 response, but only sAC activity is required for the late ERK1/2 activation phase. Our results indicate that CRH-activated CRHR1 generates cAMP from endocytic compartments. By characterizing the CRHR1 signaling response, we show a functional association between sAC-generated cAMP, ERK1/2 activation, and endosome-based GPCR signaling.

Results

sAC contributes to CRHR1-triggered cAMP response in HT22-CRHR1 cells

It is now widely accepted that sAC, which was first identified in testis, is ubiquitously expressed (Tresguerres et al., 2011). RT-PCR results confirmed that sAC mRNA was present in total mouse brain and several mouse cell lines (Fig. 1 A), including HT22 cells stably expressing CRHR1 (HT22-CRHR1 cells). Using an anti-sAC monoclonal antibody (R21), a 48-kD protein was detected by Western blot in HT22-CRHR1 cells (Fig. S1 A), and the immunoreactive band was reduced in cells transfected with a sAC-specific siRNA (Fig. 1 B).

We used the FRET-based biosensor Epac-S^{H187}, which localizes diffusely throughout the cytoplasm (Klarenbeek et al., 2015), to assess CRH-triggered cAMP production at the single-cell level in real time, without phosphodiesterase inhibitors. CRH stimulation of HT22-CRHR1 cells resulted in a rapid increase of intracellular cAMP levels that stayed elevated for at least 40 min after ligand bath application (Fig. S1 B). CRH addition produced a rapid decrease of acceptor emission (cp^{173}Venus) and a corresponding increase in donor emission (mTurquoise2), confirming that the observed changes were caused by a FRET reduction, indicating a rise in cytoplasmic cAMP concentration (Fig. S1 B).

When the tmAC-selective inhibitor 2′,5′-dideoxyadenosine (ddA) was added during the time course, the cAMP response was inhibited ($P < 0.001$ with respect to control after 5 min) but not completely blocked (Fig. 1 C). Interestingly, the sAC-specific inhibitor (Bitterman et al., 2013) 2-hydroxyestradiol (2-HE) also significantly reduced cAMP levels ($P < 0.01$ with respect to control after 5 min; Fig. 1 C). We also determined cAMP content by means of competition with [^{3}H]cAMP for PKA in HT22-CRHR1 cells preincubated with ddA or sAC-specific inhibitor KH7 (Hess et al., 2005). Both inhibitors significantly reduced the cAMP response triggered by CRH (Fig. S1 C). sAC contribution to the cAMP response triggered by CRH was also indicated by depleting cellular levels of endogenous sAC (Fig. 1 E).

We tested whether isoproterenol, an agonist of β-adrenergic receptors (which are also Gs coupled), triggered a sAC-dependent cAMP response. We observed that only the tmAC inhibitor significantly affected the cAMP increase elicited by isoproterenol (Fig. 1 D; $P < 0.001$ with respect to control and 2-HE after 5 min), showing that sAC is not a general mediator of the cAMP response generated by GPCRs in the HT22 cellular context. Collectively, our data reveal that sAC is specifically involved in the CRHR1-mediated cAMP response triggered by CRH.

We examined the blocking effect and the specificity of ddA and 2-HE on the cAMP response generated by tmACs and sAC. cAMP responses in cells stimulated with CRH or treated with the tmAC-specific activator forskolin were nearly identical in the presence of ddA (Fig. 1 F, top), reaching about a 50% inhibition at the highest inhibitor concentration assayed (200 µM). 2-HE concentrations up to 40 µM had no effect on the cAMP response generated by forskolin but caused about a 30% inhibition of the cAMP response to CRH (Fig. 1 F, bottom). These results indicate that concentrations of 100 µM ddA and 20 µM 2-HE are sufficient to assess and discriminate the contribution of sAC- and tmACs-mediated processes with our experimental approach.

Do tmACs and sAC engage different biochemical cascades?

Multiple cAMP sources may contribute to a common cAMP pool, or they may act distinctly to elicit specific cellular responses. Having established that, in addition to tmACs, sAC is necessary for the CRH-activated CRHR1 cAMP response, we decided to evaluate whether specific cAMP sources have different biological meanings in CRHR1 signaling. We investigated the role of both cAMP sources in ERK1/2 phosphorylation in HT22-CRHR1 cells. We have previously reported that ERK1/2 can be activated via CRHR1 by both G protein–dependent and –independent mechanisms (Bonfiglio et al., 2013).

The dependence of ERK1/2 phosphorylation on different cAMP sources was first assessed using a pharmacologic approach (Fig. 2 A). As reported previously, specific inhibition of tmACs with ddA attenuated only the CRH-induced early (5 min) ERK1/2 activation phase (Bonfiglio et al., 2013). Two pharmacologic inhibitors of sAC, KH7 and 2-HE, reduced pERK1/2 at the early and late time points (Figs. 2 A and S1 D). When both inhibitors were used in combination, a stronger reduction of pERK1/2 was observed at the early time point (Fig. 2 A). Furthermore, when the CRH-triggered cAMP response was analyzed with simultaneous addition of both AC inhibitors, a stronger inhibition was observed, further supporting the participation of both cAMP sources in the response (Fig. 2 B).

Next, we analyzed the time course of CRH-induced ERK1/2 phosphorylation after depleting endogenous sAC (Fig. 1 B). Knockdown of sAC significantly affected the early

Published July 11, 2016

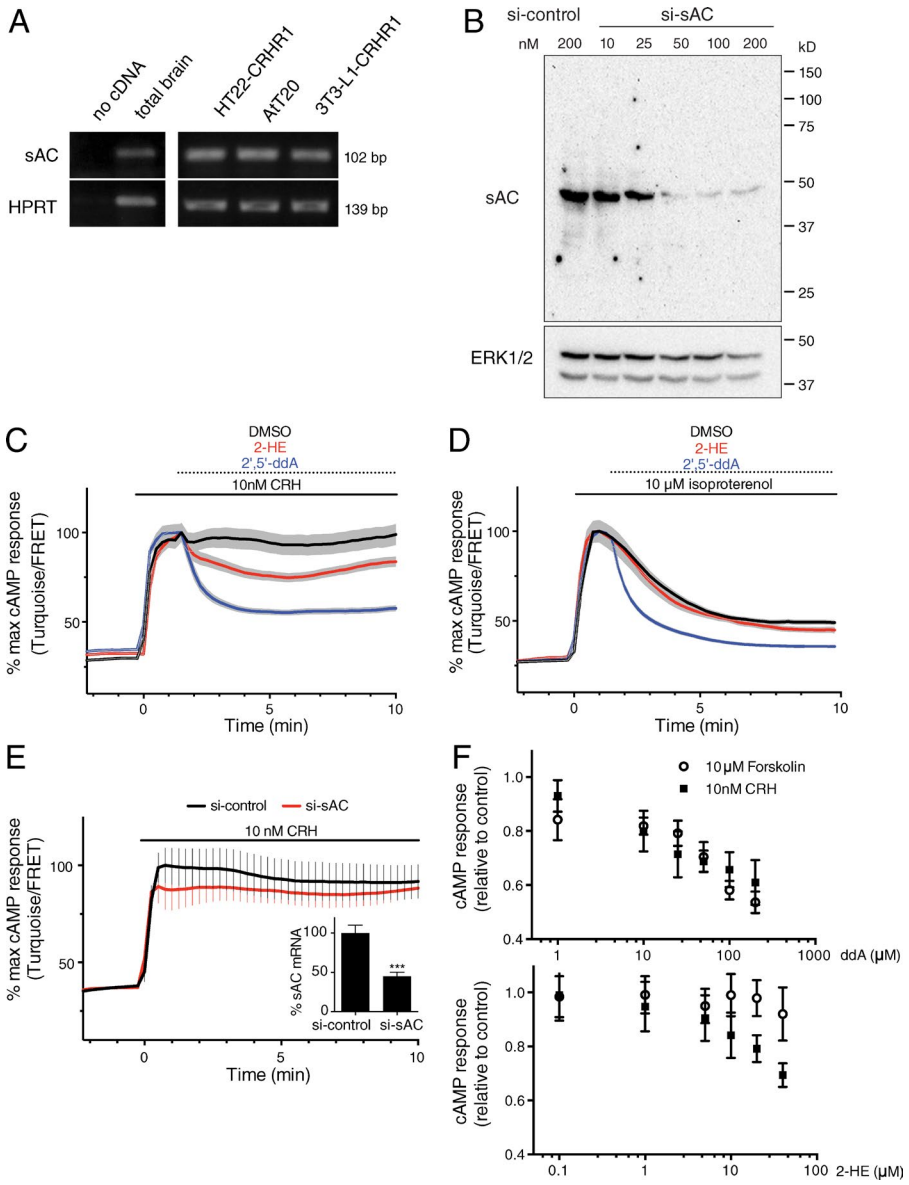

Figure 1. **Involvement of sAC in CRH-mediated cAMP response.** (A) sAC was detected by RT-PCR in total mouse brain extracts and different mouse cell lines. HPRT was used as control. (B) Depletion of sAC in HT22-CRHR1 cells transfected with siRNA against GL3 (control) or sAC. Western blot developed with sAC monoclonal antibody and total ERK1/2 as a loading control. (C–E) Time course of FRET changes was measured in single HT22-CRHR1-Epac-S^{H187} cells. Cells were stimulated at time 0 with CRH (C and E) or isoproterenol (D). tmAC-specific (100 µM ddA) or sAC-specific (20 µM 2-HE) inhibitors were added 1.5 min after stimulation. Traces are representative of three independent experiments (mean ± SEM, 20–25 cells). (E) Cells were transfected with 50 nM siRNA against GL3 (control) or sAC for 72 h. Inset shows efficiency of sAC knockdown assessed by quantitative RT-PCR normalized to HPRT (mean ± SEM, $n = 3$). ***, $P < 0.001$ by Student's t test. (F) Inhibition of cAMP response elicited by CRH or forskolin at the indicated concentrations of ddA or 2-HE. Values represent FRET change 2.5 min after inhibitor addition relative to absence of any inhibitor (mean ± SEM, 15–20 cells).

but also the late phase of CRH-mediated pERK1/2 (Fig. 2 C). In HT22-CRHR1 cells, isoproterenol triggered a biphasic ERK1/2 activation response similar to the one described in HEK293 cells (Shenoy et al., 2006). However, sAC depletion did not affect ERK1/2 phosphorylation triggered by isoproterenol in these cells (Fig. 2 C), consistent with sAC not being involved in the cAMP response to isoproterenol in HT22-CRHR1 cells (Fig. 1 D). Interestingly, in these cells, CRH-induced neurite outgrowth was blocked by KH7, but ddA had no effect, showing that the morphologic change requires sAC but not tmACs (Fig. 2 D). Together, these results show that tmACs and sAC can mediate different functions in CRH signaling.

sAC was identified in a search for B-Raf partners with a potential role in CRH signaling (Bonfiglio et al., 2013). B-Raf is the MAPK kinase kinase of the cascade leading to ERK1/2 activation and also acts as a scaffold for assembling signaling complexes. Analysis of CRH-elicited signaling mechanisms reveals that whereas sAC contributes to the cAMP response to a small extent, it has a significant role in the phosphorylation of ERK1/2. Thus, the sAC-generated cAMP pool might be biased toward activation of the ERK1/2 pathway. Consistent with the fact that CRHR1 is a Gs-coupled GPCR, the classic signal transduction mechanism involves the generation of cAMP at the plasma membrane by G protein–regulated tmACs, which is apparent in the early phase of ERK1/2 activation (Bonfiglio et al., 2013). The effect of sAC inhibition or depletion on the late phase of pERK1/2 reveals the requirement of CRH-activated sAC in the sustained signaling phase of ERK1/2 activation, suggesting that cAMP is required for ERK1/2 response in the receptor endocytosis-dependent phase.

sAC is involved in CRH signaling in AtT20 corticotrophs but not in 3T3L1-CRHR1 cells

Is sAC a specific component of CRHR1 signaling in a hippocampal neuronal context, or does it have a general role in CRHR1 function? To answer this question, we selected the mouse pituitary-derived corticotroph cell line AtT20 as a second physiologically relevant context of CRH action. In AtT20 cells, CRHR1 (Peeters et al., 2004) and sAC (Fig. 1 A) are endogenously expressed, and CRH elicits a transient increase in cAMP levels and activates ERK1/2 (Fig. S2, A and B).

Published July 11, 2016

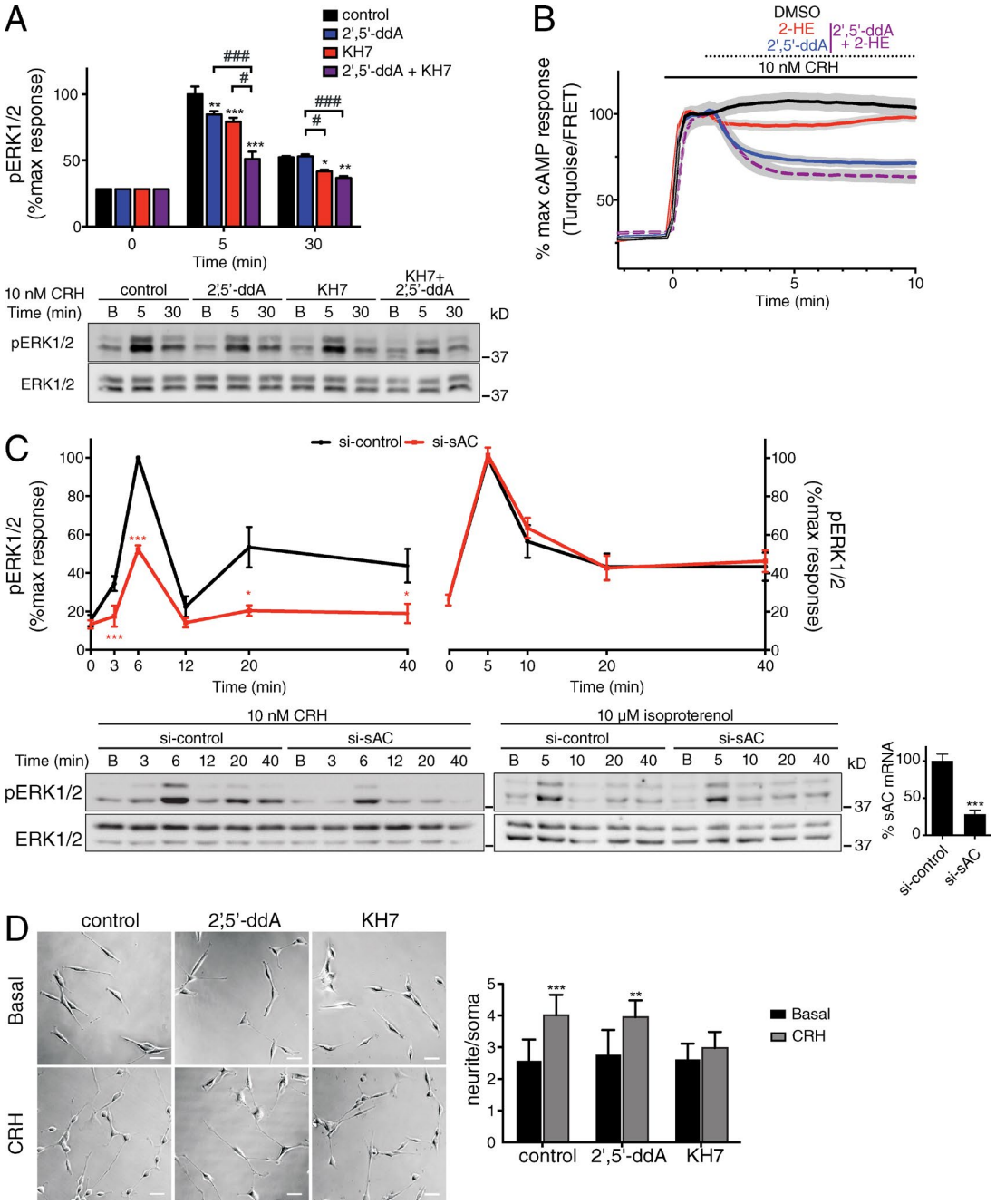

Figure 2. **sAC-generated cAMP has a specific role in CRHR1 signaling.** (A–C) pERK1/2 and total ERK1/2 were measured in HT22-CRHR1 cells stimulated with CRH or isoproterenol for the indicated time points. Results are expressed as the percentage of maximum pERK1/2. (A) Cells were preincubated with vehicle (control) or sAC-specific (7.5 µM KH7) or tmAC-specific (100 µM ddA) inhibitors (mean ± SEM, $n = 4$). Two-way analysis of variance followed by Tukey's test: *, $P < 0.05$; **, $P < 0.01$; ***, $P < 0.001$ with respect to control; #, $P < 0.05$; ###, $P < 0.01$ between indicated treatments. (B) Time course of FRET changes was measured in single HT22-CRHR1-Epac-S^{H187} cells. Cells were stimulated at time 0 with CRH. When indicated, tmAC-specific (100 µM ddA) or sAC-specific (20 µM 2-HE) inhibitors were added. Traces are representative of three independent experiments (mean ± SEM, 20–25 cells). (C) Cells were transfected with 50 nM siRNA against GL3 (control) or sAC for 72 h before stimulation with CRH or isoproterenol (mean ± SEM, $n = 3$). Student's t test was performed for each time point. *, $P < 0.05$; ***, $P < 0.001$. Efficiency of sAC knockdown assessed by quantitative RT-PCR normalized to HPRT is shown (mean ± SEM, $n = 3$). ***, $P < 0.001$ by Student's t test. (D) CRH neurogenic effect in HT22-CRHR1 cells after 20-h treatment was evaluated in the presence of vehicle (control) or tmAC-specific (50 µM ddA) or sAC-specific (7.5 µM KH7) inhibitors. A representative photograph is shown. Bar, 50 µm. Neurite outgrowth was quantified by repeated-measures one-way analysis of variance followed by Tukey's test ($n = 3$). ***, $P < 0.001$; **, $P < 0.01$ with respect to basal.

To determine the involvement of different cAMP sources, we analyzed ERK1/2 activation in response to CRH, which is critical for *Pomc* expression (Kovalovsky et al., 2002) and is mediated by cAMP (Van Kolen et al., 2010). Using inhibitors, we found that tmAC-specific ddA, as well as two sAC-selective inhibitors, 2-HE and KH7, impaired CRH-mediated ERK1/2 phosphorylation (Fig. 3 A). sAC knockdown also significantly reduced CRH-triggered pERK1/2 levels, confirming that sAC participates in CRHR1 signal transduction in AtT20 cells (Fig. 3 B). In contrast, depletion of sAC had no effect on

Published July 11, 2016

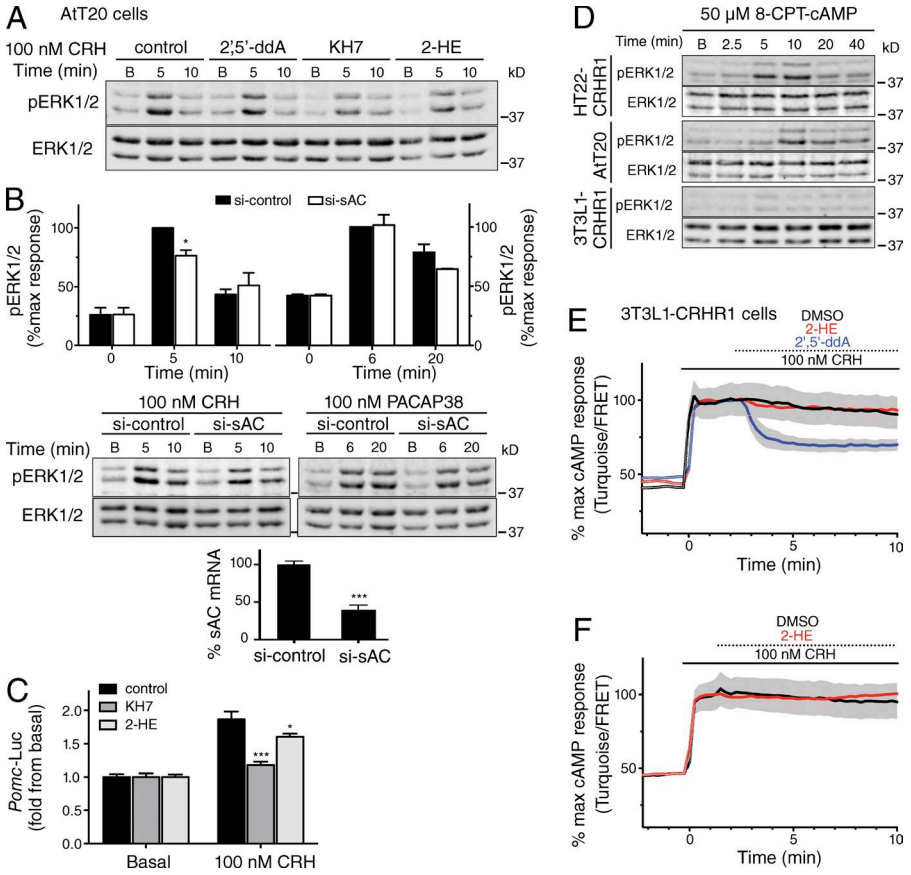

Figure 3. **CRH responses in AtT20 and 3T3L1-CRHR1 cells.** (A) pERK1/2 and total ERK1/2 were measured in AtT20 cells preincubated with vehicle (control) or tmAC-specific (50 µM ddA) or sAC-specific (7.5 µM KH7 or 10 µM 2-HE) inhibitors and stimulated with CRH. (B) pERK1/2 and total ERK1/2 were measured in AtT20 cells transfected with 50 nM siRNA against GL3 (control) or sAC and stimulated with CRH or PACAP38. Results are expressed as the percentage of maximum pERK1/2 (mean ± SEM, n = 3). *, P < 0.05 by Student's t test. Efficiency of sAC knockdown assessed by quantitative RT-PCR normalized to HPRT is shown (mean ± SEM, n = 3). ***, P < 0.001 by Student's t test. (C) Response to CRH in AtT20 cells transiently transfected with *Pomc*–Luc and pretreated with 7.5 µM KH7 or 10 µM 2-HE. Each value was normalized to β-Gal activity (mean ± SEM, n = 4 of one representative of three independent experiments with similar results). ***, P < 0.001; *, P < 0.05 with respect to control by two-way analysis of variance followed by Tukey's test. (D) pERK1/2 and total ERK1/2 of HT22-CRHR1, AtT20, or 3T3L1-CRHR1 cells treated with 8-CPT-cAMP. (E,F) 3T3L1-CRHR1 cells expressing Epac-S^{H187} were stimulated at time 0 with CRH. (F) Cells were transfected with sACt-HA. When indicated, 100 µM ddA or 20 µM 2-HE was added. Time course of FRET changes were measured in single cells. Traces are representative of three independent experiments (mean ± SEM, 20–30 cells).

PACAP38-mediated ERK1/2 activation (Figs. 3 B and S2 C). Given that PACAP38 also signals through a class B GPCR that generates a cAMP response (Fig. S2 A), these results further highlight that sAC is a specific component of CRHR1 signaling.

We next tested whether sAC was involved in the CRH-mediated activation of *Pomc*, a key CRH target gene in corticotroph cells for HPA axis activation. The transcriptional activity of a *Pomc*–Luc reporter construct (Liu et al., 1992) was significantly decreased in cells pretreated with sAC inhibitors before CRH stimulation, whereas no effects on basal activities were observed (Fig. 3 C). These findings are consistent with the participation of sAC in a second signaling scenario and suggest that sAC has a key role for CRHR1 action.

We used the mouse fibroblast 3T3L1 cell line stably expressing CRHR1 (3T3L1-CRHR1), which endogenously expresses sAC (Fig. 1 A), as a third cellular context to explore a role of sAC in CRHR1 signaling. Treatment with the cell membrane–permeable cAMP analog 8-CPT-cAMP enhances ERK1/2 phosphorylation in cells in which ERK1/2 activation is dependent on increased cAMP levels. ERK1/2 response to 8-CPT-cAMP in the three cell lines was determined (Fig. 3 D). Although CRH activated ERK1/2 and CREB in 3T3L1-CRHR1 cells (Fig. S2 D), pERK1/2 was not linked to increased cAMP levels in this system, unlike in ATt20 and HT22-CRHR1 cells (Fig. 3 D).

We tested the participation of sAC in 3T3L1-CRHR1 cells by measuring the CRH-mediated cAMP response using the FRET-based biosensor. CRH stimulation triggered a rapid and sustained increase in cAMP levels. Interestingly, whereas the tmAC-selective inhibitor ddA attenuated the cAMP response, the addition of sAC-specific inhibitor 2-HE did not have a significant effect on the cAMP time course (Fig. 3 E). To rule out the possibility that this result was caused by low sAC expression levels, the experiment was also performed with overexpression of the highly active sACt isoform, with similar results (Fig. 3 F).

CRH-activated CRHR1 has been shown to trigger an increase in calcium in several cellular contexts (Kovalovsky et al., 2002; Gutknecht et al., 2009; Bonfiglio et al., 2013). Because calcium activates sAC (Jaiswal and Conti, 2003; Carlson et al., 2007; Kleinboelting et al., 2014), we asked whether a CRHR1-dependent calcium response was present in 3T3L1-CRHR1 cells. Using Fluo-4 calcium indicator, we verified that, upon CRH stimulation, there was a calcium increase that could be completely blocked with the extracellular calcium chelator EGTA (Fig. S2 E). In conclusion, despite the fact that CRH-driven responses in 3T3L1-CRHR1 and HT22-CRHR1 cells are comparable in terms of cAMP (Fig. 1 C and Fig. 3, E and F) and calcium responses (Bonfiglio et al., 2013), sAC is not involved in cAMP generation in 3T3L1-CRHR1 cells. These findings suggest that the involvement of sAC is dependent on the cellular context and that there is a functional association between the sAC-generated cAMP pool and the ERK1/2 pathway.

CRH-stimulated sAC activates PKA and EPACs

Both PKA and EPACs (cAMP-stimulated guanine nucleotide exchange factors) can trigger the ERK1/2 pathway (Kawasaki et al., 1998). It has been shown that sAC-generated cAMP signals through PKA during capacitation in mammalian sperm (Wertheimer et al., 2013), during leukocyte transendothelial migration (Watson et al., 2015), and in H_2O_2-stimulated airway epithelia (Ivonnet et al., 2015), whereas the sAC-EPAC-

Published July 11, 2016

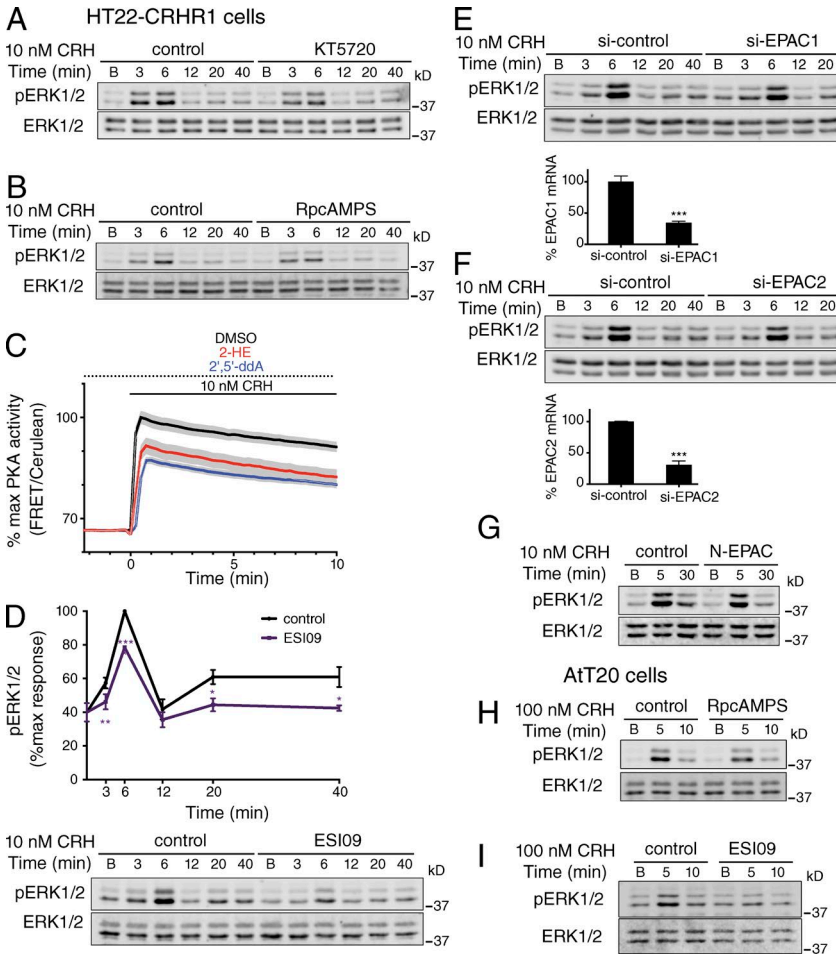

Figure 4. **sAC effectors in HT22-CRHR1 and AtT20 cells.** (A,B,D–F) pERK1/2 and total ERK1/2 were measured in HT22-CRHR1 cells stimulated with CRH for the indicated time points. (A, B, and D) Cells preincubated with vehicle (control), PKA inhibitors (A: 700 nM KT5720; B: 75 µM RpcAMPS), or EPAC-specific inhibitor (5 µM ESI09) were stimulated with CRH. In D, results are expressed as the percentage of maximum pERK1/2 after stimulation under control conditions (mean ± SEM, $n = 3$). *, $P < 0.05$; **, $P < 0.01$; ***, $P < 0.001$ by Student's t test. (C) HT22-CRHR1 cells stably expressing AKAR4 were preincubated with tmAC-specific (100 µM ddA) or sAC-specific (20 µM 2-HE) inhibitors and stimulated with CRH at time 0. Time course of FRET changes was measured in single cells. Traces are representative of three independent experiments (mean ± SEM, 20–25 cells). (E and F) Cells were transfected with 50 nM siRNA against GL3 (control), EPAC1, or EPAC2 for 72 h before CRH stimulation. Efficiency of EPAC1 or EPAC2 knockdown assessed by quantitative RT-PCR normalized to HPRT is shown (mean ± SEM, $n = 3$). ***, $P < 0.001$ by Student's t test. (G) Cells were transfected with EPAC1 (control) or dominant negative N-EPAC 48 h before CRH stimulation. (H and I) pERK1/2 and total ERK1/2 were measured in AtT20 cells preincubated with vehicle (control), PKA inhibitor (75 µM RpcAMPS; H), or EPAC inhibitor (10 µM ESI09; I) and stimulated with CRH for the indicated times.

Rap1 axis has been associated with cell proliferation in prostate and breast cancer cells (Flacke et al., 2013; Appukuttan et al., 2014; Onodera et al., 2014).

In HT22-CRHR1 cells, pharmacologic inhibition of PKA reduced CRH-mediated early ERK1/2 activation, without affecting late time points (Fig. 4, A and B). To study PKA activation directly, we expressed the FRET-based PKA activity sensor AKAR4 (Allen and Zhang, 2006; Depry et al., 2011). Preincubation with ddA as well as 2-HE significantly prevented CRH-triggered PKA activation (Fig. 4 C). Thus, cAMP generated through tmAC and sAC contributes to PKA activity in CRH-stimulated HT22-CRHR1 cells.

To determine the role of EPACs on CRH action, we used the EPAC1 and EPAC2 inhibitor ESI09 (Zhu et al., 2015) at its lowest effective concentration to avoid reported nonspecific effects (Rehmann, 2013). Preincubation with ESI09 strongly reduced CRH-mediated pERK1/2 at both early and late time points (Fig. 4 D). Genetic silencing of EPAC1 and EPAC2 and transfection with the dominant-negative N-EPAC also diminished ERK1/2 activation (Fig. 4, E–G). The modest impact of EPAC knockdown may result from incomplete protein depletion. Alternatively, the stronger action of ESI09 or N-EPAC may result from nonspecific effects of these treatments. Therefore, EPACs participate in the activation of ERK1/2 in response to CRH in the hippocampal neuronal context. Moreover, the involvement of EPACs in the sustained phase of ERK1/2 activation further supports that the endocytosis-dependent mechanism of ERK1/2 activation requires cAMP.

In AtT20 cells, CRH-induced ERK1/2 activation was slightly decreased in the presence of the PKA inhibitor RpcAMPS (Fig. 4 H). Treatment with the EPAC inhibitor impaired pERK1/2 in response to CRH (Fig. 4 I). Thus, in line with previous studies (Van Kolen et al., 2010), the main cAMP effector underlying CRH-mediated ERK1/2 activation in AtT20 cells is EPAC. Collectively, these results indicate that sAC-generated cAMP does not signal preferentially through a specific cAMP effector, being able to activate both PKA and EPAC in response to CRH.

Endocytosis-dependent cAMP is generated in response to CRH

CRHR1–β-arrestins interactions are involved in CRHR1 desensitization (Perry et al., 2005; Holmes et al., 2006; Oakley et al., 2007). We have shown previously that, upon ligand stimulation, CRHR1 is internalized and stays in endocytic compartments 30 min after CRH addition. We examined agonist-induced CRHR1 internalization in HT22-CRHR1 cells. CRH activation promoted a fast internalization of the receptor, with a time course that overlapped that of cAMP production: a significant fraction of CRHR1 was internalized after 5 min and remained constant for at least 30 min of CRH stimulation (Fig. 5 A). The fact that both the early and late phases of ERK1/2 activation were affected when sAC activity was inhibited or silenced led us to postulate that CRHR1 endocytosis and sAC activity may be linked. To test this hypothesis, we used two experimental approaches to inhibit endocytosis and measured the time course of cAMP accumulation mediated by CRH with the FRET-based biosensor.

Published July 11, 2016

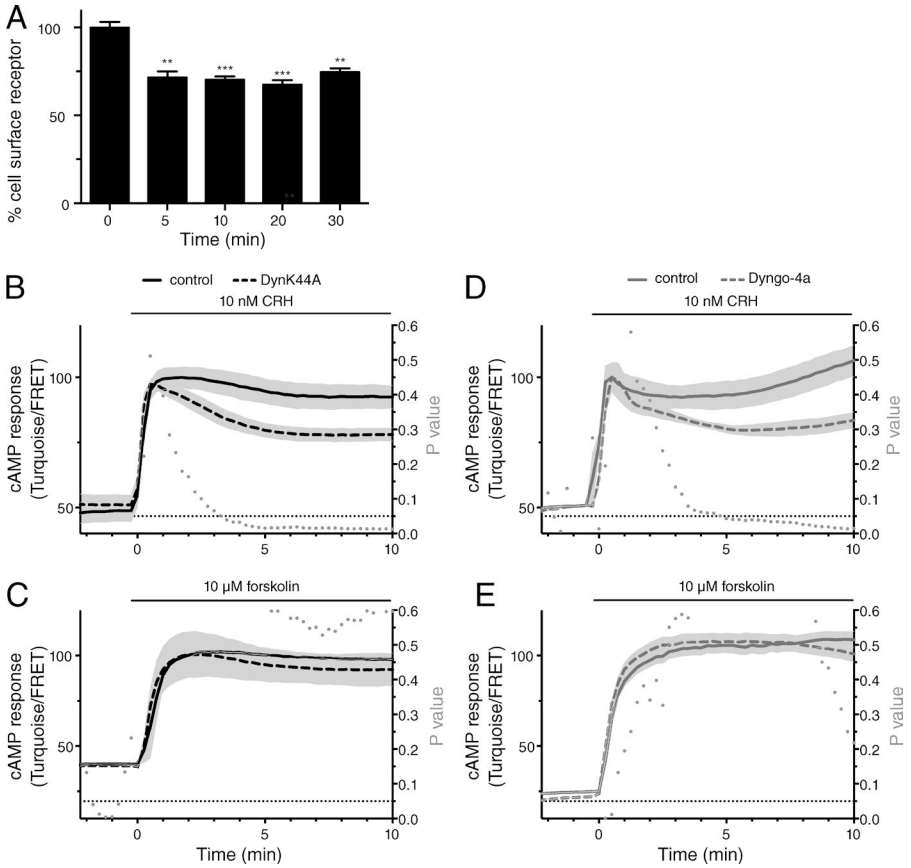

Figure 5. **cAMP response to CRH depends on endocytosis.** (A) Agonist-induced CRHR1 internalization was analyzed by fluorescence flow cytometry at the indicated time points after stimulation by 10 nM CRH in HT22-CRHR1 cells. Fluorescence at time 0 was defined as 100% (mean ± SEM, n = 4, 10,000 cells/condition). ***, P < 0.001; **, P < 0.01 with respect to basal by one-way analysis of variance followed by Tukey's test. HT22-CRHR1-Epac-S^{H187} cells were stimulated at time 0 with CRH (B and D) or forskolin (C and E). (B and C) Cells were transfected with pcDNA3 (control) or DynK44A 48 h before stimulation. (D and E) Cells were preincubated with vehicle (control) or 30 μM Dyngo-4a 15 min before stimulation. Time course of FRET changes was measured in single cells (mean ± SEM, n = 4). Student's t test was performed for each time point. P values in gray; P = 0.05 is indicated with a dotted line.

First, we used a genetic approach, expressing a dominant-negative mutant of dynamin (DynK44A) that is required for later stages of clathrin-dependent endocytosis. DynK44A blocked CRHR1 internalization upon ligand stimulation (Fig. S3, A and B) and the sustained ERK1/2 activation phase in HT22-CRHR1 cells (Bonfiglio et al., 2013). Cells transfected with DynK44A showed a diminished cAMP response compared with control cells (Fig. 5 B). Next, we followed a pharmacologic approach using Dyngo-4a, which chemically inhibits dynamin's GTPase activity, blocking endocytosis (Fig. S3, A and C). As in cells expressing DynK44A, the cAMP response to CRH was impaired by Dyngo-4a treatment, showing a profile similar to the one observed with DynK44A (Fig. 5 D).

The early increase of CRH-mediated cAMP accumulation did not seem to be affected by dynamin-deficient mutant or Dyngo-4a. The differences in the time course of the cAMP response when endocytosis was inhibited were significant 3.5 min after CRH stimulation (Fig. 5, B and D), in line with fast CRHR1 endocytosis (Fig. 5 A; Kotowski et al., 2011; Bonfiglio et al., 2013). Importantly, DynK44A expression or Dyngo-4a treatment did not significantly affect the cAMP response elicited by receptor-independent activation of adenylyl cyclases with forskolin (Fig. 5, C and E), confirming that the effect of endocytosis inhibition required pathway stimulation by the activated receptor.

Changes in the CRH-dependent calcium response cannot be ascribed to a decreased cAMP response in these cells because a similar calcium response was observed in both control and DynK44A-expressing cells (Fig. S3 D). Thus, inhibition of endocytosis produces a significant decrease of cellular cAMP accumulation mediated by CRHR1.

For the class B GPCR PTHR, PTH-triggered cAMP production continues after internalization by a mechanism dependent on receptor interaction with β-arrestins and prolonged ERK1/2 signaling (Feinstein et al., 2011). We investigated whether activated ERK1/2 was involved in the CRH-cAMP response in HT22-CRHR1 cells. When cells were pretreated with the MEK1/2 inhibitor U0126, a complete blockage of CRH-activated ERK1/2 was observed (Fig. S3 E). However, no differences were found between control and treated cells in the CRH-mediated cAMP response (Fig. S3 F), indicating that cAMP generated by CRH-activated CRHR1 does not depend on ERK1/2 activation.

sAC activity is essential for endocytosis-dependent CRHR1 signaling

We investigated the cAMP source involved in CRHR1 signaling after internalization, combining ACs inhibitors with endocytosis blockage. HT22-CRHR1-Epac-S^{H187} cells transfected with an empty vector or DynK44A mutant (coexpressed with mCherry) were mixed so that both types of cells could be treated, CRH-stimulated, and analyzed in the same microscope field (Fig. 6 A). When cells were preincubated with vehicle or the tmAC inhibitor ddA, cAMP levels were reduced faster in cells transfected with DynK44A compared with neighboring control cells. However, preincubation with the sAC inhibitor 2-HE led to a loss of the endocytosis effect on the cAMP response to CRH (Fig. 6 B). This result strongly suggests that the endocytosis-dependent component of the cAMP response is largely dependent on sAC activity. Importantly, 2-HE did not affect CRH-activated CRHR1 endocytosis, as shown by flow cytometry analysis and subcellular localization of CRHR1-GFP (Fig. 6, C and D).

Published July 11, 2016

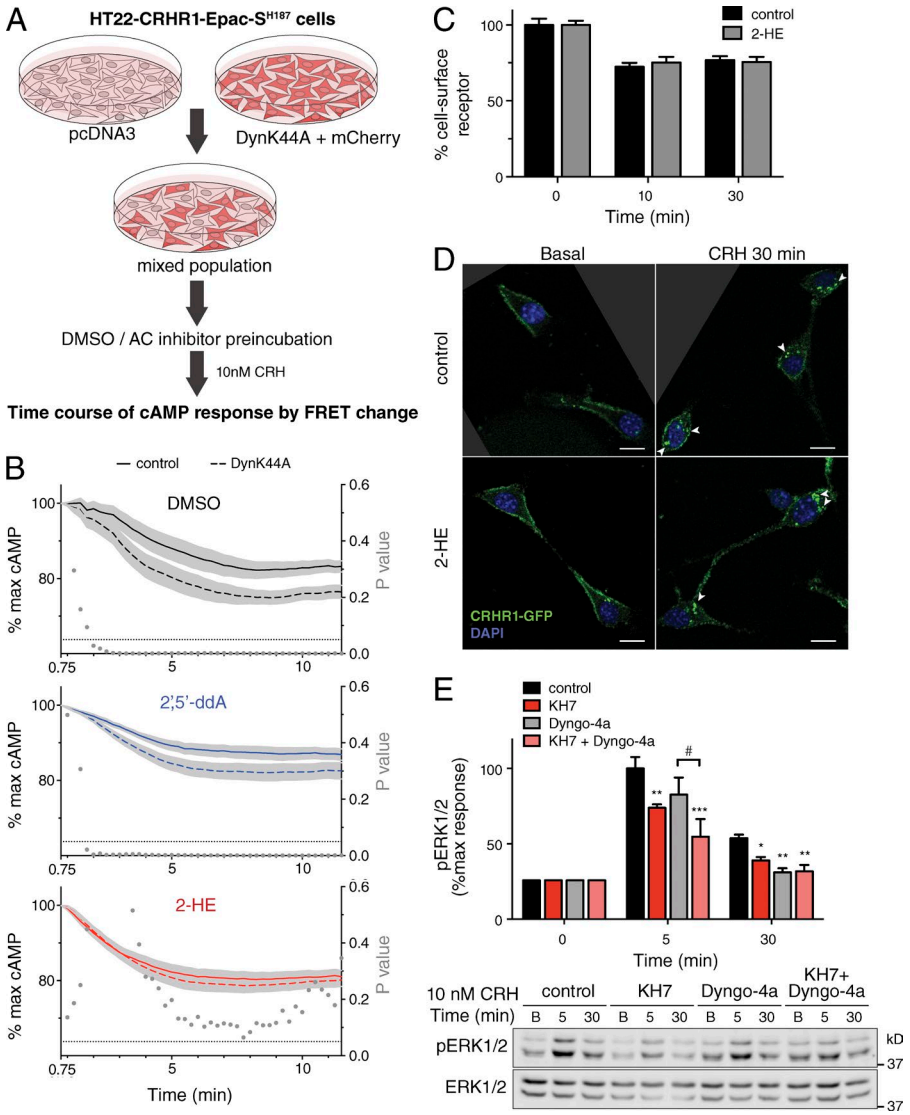

Figure 6. **sAC is critical for endosome-generated cAMP in response to CRH.** (A) Schematic representation of the experimental design. HT22-CRHR1-Epac-S^{H187} cells transfected with pcDNA3 (control) or DynK44A plus mCherry for 48 h were pretreated with vehicle (DMSO) or tmAC-specific (100 µM ddA) or sAC-specific (20 µM 2-HE) inhibitors and stimulated with 10 nM CRH. (B) Time course of FRET changes was measured in single cells. The cAMP response is expressed as the percentage of maximum FRET signal obtained in each condition assayed after stimulation (mean ± SEM, *n* = 7). Student's *t* test was performed for each time point. P values in gray; P = 0.05 is indicated with a dotted line. (C and D) Effect of 2-HE on agonist-induced CRHR1 internalization analyzed by fluorescence flow cytometry (C) and cMyc-GFP-CRHR1 subcellular distribution (D). HT22-CRHR1 cells preincubated with vehicle (control) or 20 µM 2-HE were stimulated with 10 nM CRH for the indicated times. (C) Fluorescence measured at time 0 was defined as 100% (mean ± SEM, *n* = 4, 10,000 cells/condition). (D) Representative images obtained for each condition. Arrowheads point to internalized GFP clusters. Bars, 5 µM. (E) pERK1/2 and total ERK1/2 were measured in HT22-CRHR1 cells preincubated with vehicle (control) or sAC-specific (7.5 µM KH7) or endocytosis-specific (30 µM Dyngo-4a) inhibitors and stimulated with CRH. Results are expressed as the percentage of maximum pERK1/2 (mean ± SEM, *n* = 4). Two-way ANOVA followed by Tukey's test: *, P < 0.05; **, P < 0.01; ***, P < 0.001 with respect to control; #, P < 0.05 between indicated treatments.

The differences between CRH-elicited cAMP responses in the presence or absence of a functional endocytosis machinery can be measured for at least 20 min (Fig. S3 G). As a control, when ddA was added after 10 min, cAMP responses were reduced, but the difference in cAMP levels between control and DynK44A cells was maintained (Fig. S6 H). This further indicates that tmACs are still active but are not critical for endocytosis-dependent cAMP generation.

The effect of sAC inhibition and endocytosis blockage on ERK1/2 activation was assessed (Fig. 6 E). As previously shown (Fig. 2 A), preincubation with the sAC-specific inhibitor KH7 diminished ERK1/2 activation at early and late time points, whereas the endocytosis inhibitor Dyngo-4a caused a significant reduction of late pERK1/2. Simultaneous inhibition of sAC activity and endocytosis resulted in lower ERK1/2 activation at the early time point compared with Dyngo-4a treatment alone, showing that sAC plays a role in the early endocytosis-independent phase. Remarkably, both treatments, separately or combined, reduced late pERK1/2 to a similar extent, suggesting that sAC activity and endocytosis are involved in the same mechanism that operates at the second signaling phase.

CRH-triggered response depends on sAC modulators: calcium and bicarbonate

sAC is stimulated by calcium (Jaiswal and Conti, 2003; Carlson et al., 2007; Kleinboelting et al., 2014), which may regulate sAC activity in neurons (Wu et al., 2006; Corredor et al., 2012). In HT22-CRHR1 cells, CRH elevates intracellular calcium (Bonfiglio et al., 2013). To monitor cAMP and calcium responses simultaneously, we used the FRET-based cAMP sensor in combination with a genetically encoded red calcium indicator, REX-GECO1 (Wu et al., 2014). CRH stimulation resulted in rapid and synchronized responses of both second messengers, albeit with different profiles: intracellular calcium increased sharply upon stimulation and returned to basal levels after 60 s, whereas cAMP levels were sustained (Fig. 7, A and B). Preincubation with the cell-permeable calcium chelator BAPTA-AM reduced pERK1/2 at both early and late time points (Fig. S4 A), showing that calcium is critical for the ERK1/2 response. Remarkably, the ERK1/2 activation profile in the presence of calcium chelators was reminiscent of the one silencing sAC (Fig. 2 C).

In addition to sAC, two tmACs (AC1 and AC8) are also positively regulated by calcium (Willoughby and Cooper, 2007). In accordance with our previous study that the tmAC-specific

Published July 11, 2016

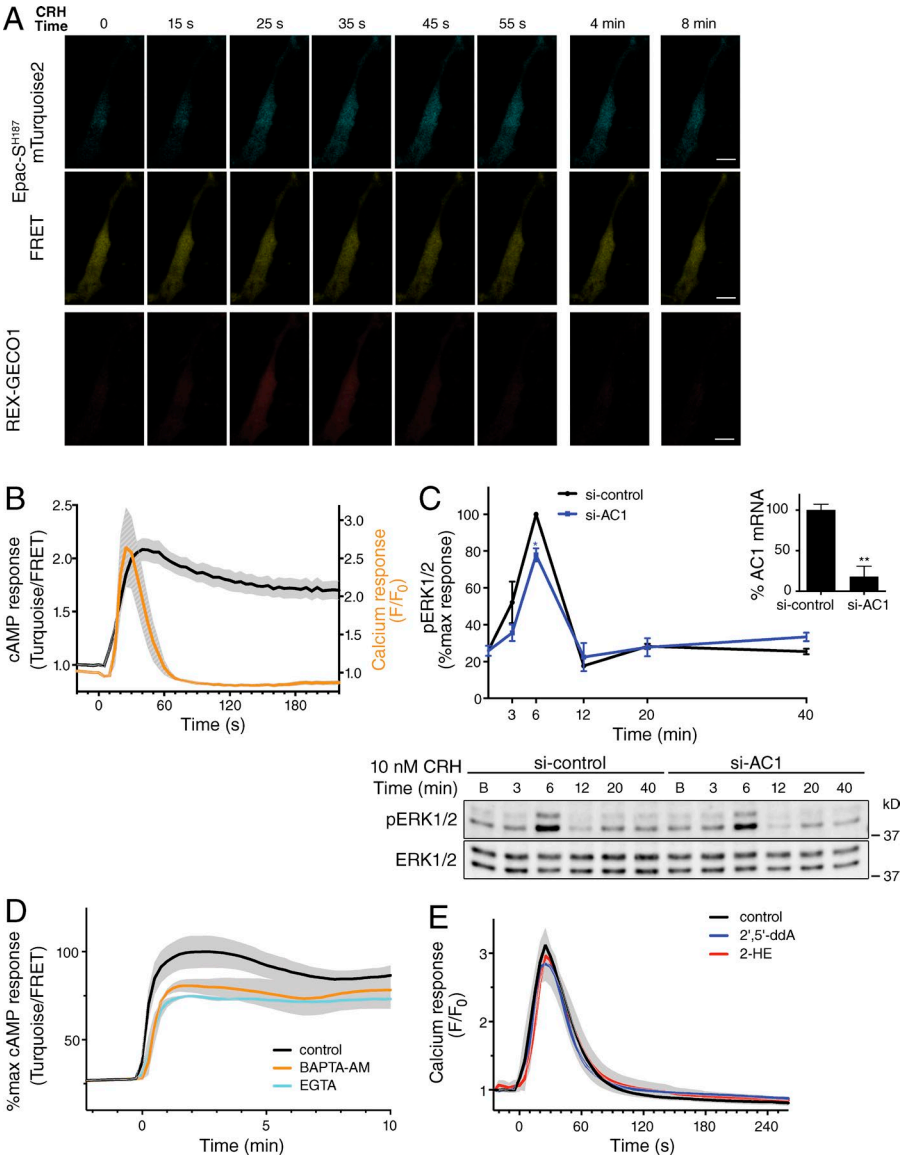

Figure 7. **CRH-triggered calcium response regulates cAMP.** (A and B) HT22-CRHR1 cells cotransfected with Epac-S^{H187} and REX-GECO1 were stimulated with 100 nM CRH. (A) Representative images for each signal. Bar, 5 µm. (B) Time course of FRET changes (black trace) or REX-GECO1 fluorescence (orange trace). Data: mean ± SEM, 14 cells. (C) pERK1/2 and total ERK1/2 were measured in HT22-CRHR1 cells transfected with 50 nM siRNA against GL3 (control) or AC1 and stimulated with CRH. Results are expressed as the percentage of maximum pERK1/2 after stimulation under control conditions (mean ± SEM, $n = 3$). *, $P < 0.05$; **, $P < 0.01$ by Student's t test. Efficiency of AC1 knockdown assessed by quantitative RT-PCR normalized to HPRT is shown (mean ± SEM, $n = 3$). **, $P < 0.01$ by Student's t test. (D) HT22-CRHR1-Epac-S^{H187} cells preincubated with vehicle (control), 5 µM BAPTA-AM, or 500 µM EGTA were stimulated at time 0 with CRH. Time course of FRET changes was measured in single cells (mean ± SEM, $n = 3$). (E) Calcium response was determined in HT22-CRHR1 cells pretreated with tmAC-specific (100 µM ddA) or sAC-specific (20 µM 2-HE) inhibitors, loaded with Fluo-4-AM, and stimulated at time 0 with 100 nM CRH (mean ± SEM, $n = 3$).

inhibitor ddA affected only the early phase of ERK1/2 activation (Bonfiglio et al., 2013), knockdown of AC1 significantly diminished pERK1/2 at early time points but did not alter the sustained phase (Fig. 7 C). We could not detect AC8 expression in this system or an effect on the ERK1/2 response using an siRNA against AC8 (Fig. S4, B and C).

If CRH-mediated calcium influx were critical for sAC activation, a reduced cAMP response would be expected when CRH-elicited calcium increase is blocked. CRH-triggered cAMP response was diminished to a similar extent by extracellular EGTA and cell-permeable BAPTA-AM calcium chelators in pretreated HT22-CRHR1 cells (Fig. 7 D), indicating that the cAMP response depends, at least partially, on a calcium-sensitive mechanism. Notably, the calcium response elicited by CRH was not altered in HT22-CRHR1 cells preincubated with ddA or 2-HE (Fig. 7 E), suggesting that calcium, required for sAC activity, would not depend on cAMP stimulation by CRH-activated CRHR1.

Next, we examined the effect of the sAC-specific modulator bicarbonate (Steegborn et al., 2005; Kleinboelting et al., 2014) on the ERK1/2 response to CRH. Bicarbonate concentration in the culture medium used to grow cells and perform experiments was 25 mM, which reproduces the bicarbonate concentration in vivo. When we stimulated HT22-CRHR1 cells with CRH in bicarbonate-free medium, ERK1/2 activation was strongly attenuated. Strikingly, the late phase of ERK1/2 activation almost disappeared (Fig. 8 A).

Pharmacologic blockage of anion exchangers with stilbene derivative DIDS modulated bicarbonate levels and sAC activity (Choi et al., 2012). Recently, DIDS has been shown to inhibit sAC by competition with bicarbonate (Kleinboelting et al., 2014). CRH-mediated pERK1/2 in the presence of DIDS resulted in a modest decrease of the ERK1/2 response at early time points and almost null ERK1/2 activation at late time points (Fig. 8 B). By either silencing sAC (Fig. 2 C) or blocking bicarbonate transport (Fig. 8 B), we found reduced CRH-dependent ERK1/2 activation, which provides further evidence for a role of bicarbonate-sensitive sAC activity in CRHR1 signaling in HT22-CRHR1 cells.

Collectively, these data are consistent with a mechanism in which CRH-activated sAC is regulated by calcium and bicarbonate and support the notion of sAC activity being required in the late phase of ERK1/2 activation.

Published July 11, 2016

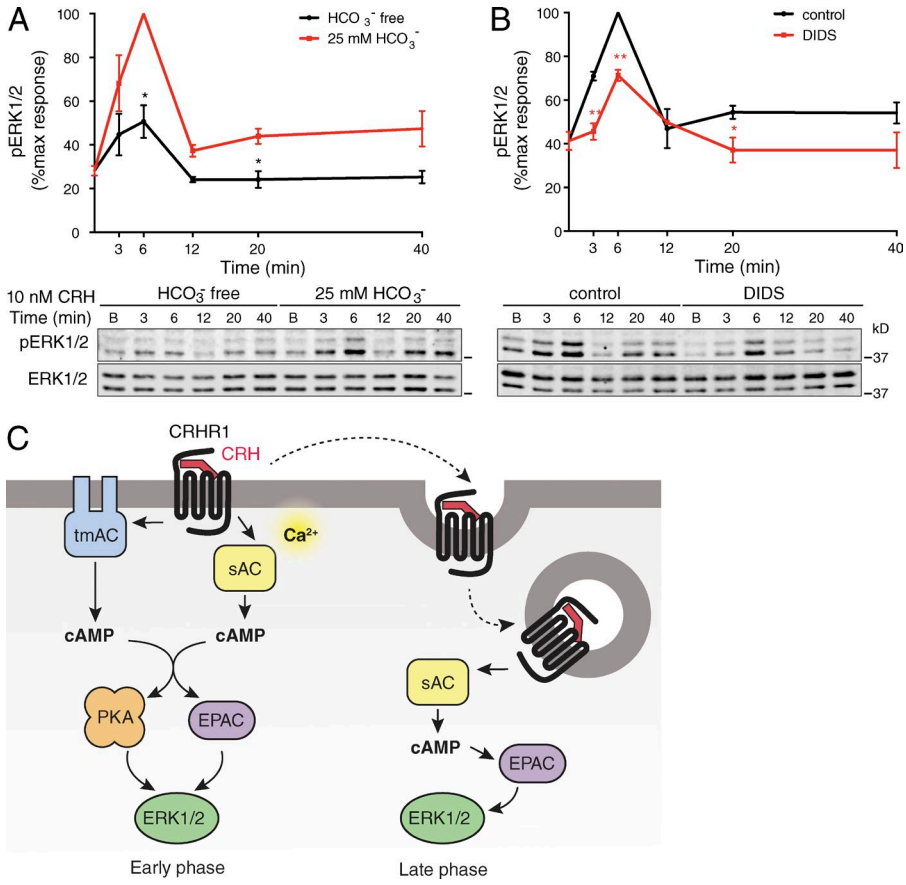

Figure 8. **CRH-elicited cAMP response depends on bicarbonate.** (A) HT22-CRHR1 cells were stimulated with CRH in HCO_3^--free or 25 mM HCO_3^- DMEM. (B) HT22-CRHR1 cells preincubated with vehicle (control) or anion channel blocker DIDS were stimulated with CRH. pERK1/2 and total ERK1/2 were measured and expressed as the percentage of maximum pERK1/2 under control conditions (mean ± SEM, $n = 3$). *, $P < 0.05$; **, $P < 0.01$ by Student's t test. (C) Proposed model: CRH-activated CRHR1 at the plasma membrane generates cAMP and intracellular calcium increase. G protein–dependent tmACs and calcium-activated sAC contribute to cAMP generation, which engages PKA and EPAC in acute ERK1/2 activation (early phase). Rapid CRHR1 internalization leading to G protein–independent sustained ERK1/2 activation (late phase) requires cAMP generated through sAC via EPAC.

Discussion

In this study, we demonstrate that sAC is a second source of cAMP in CRHR1 signaling mechanisms elicited by CRH in two physiologically relevant contexts of CRH action. We show that cAMP generated by sAC contributes to the overall cAMP response and that it is critical for ERK1/2 activation upon CRH treatment.

Our work in the hippocampal neuronal context, HT22 cells, also indicates that CRH-activated CRHR1 continues to generate cAMP from endocytic compartments, as recently demonstrated for several GPCRs (Irannejad and von Zastrow, 2014; Vilardaga et al., 2014). The study of CRH-activated CRHR1 uncovers a previously unanticipated link between sAC and endosome-based GPCR signaling. These findings revise the canonical model in which GPCR-elicited cAMP production relies solely on tmACs.

A role of sAC in GPCR signaling is just beginning to emerge; only scarce and indirect evidence has been provided so far (Halm et al., 2010; Ivonnet et al., 2015). sAC is unique among the ACs in being activated by bicarbonate and calcium (Jaiswal and Conti, 2003; Han et al., 2005). Moreover, unlike tmACs, sAC has no membrane-spanning domains and is distributed throughout the cell. Despite growing evidence that sAC might be responsible for cAMP-mediated functions previously attributed to tmACs, little is known about the mechanisms involved. Here, we identified a key role of CRHR1-induced calcium for sAC activation with both PKA and EPAC effector proteins downstream of sAC (Fig. 8 C).

In HT22-CRHR1 cells, PKA is involved only in the early ERK1/2 activation phase, whereas EPAC participates in both phases. In the neuroendocrine cell model AtT20, ERK1/2 activation was dependent on both PKA and EPAC. Notably, cAMP and ERK1/2 responses to CRH are short-lived in these cells, resembling the acute phase of pERK1/2 in HT22-CRHR1. Although our data do not rule out an endosome-based CRHR1 signaling mechanism in AtT20 cells, which remains to be explored, they show that ERK1/2 activation requires sAC.

How is sAC physically integrated in signaling complexes at specific cellular locations? Recent work describes a complex assembled by ezrin, an A-kinase anchoring protein that holds sAC at the plasma membrane (Watson et al., 2015). A systematic analysis of sAC interactions will provide insight into specific functions of spatially restricted cAMP pools in cellular responses.

We show that sAC is not a general mediator of GPCRs that activate ERK1/2 downstream of cAMP. Alternative sources of cAMP involved in signaling generated by GPCRs from the endocytic pathway have not yet been explored. Even though sAC is likely to be engaged by a variety of GPCRs, its involvement may depend on specific features of the integral cellular response rather than just the mode of signaling or the cellular context.

β-Arrestins and CRHR1 internalization contribute to ERK1/2 activation in response to CRH, suggesting sustained CRHR1 signaling in endosomes (Bonfiglio et al., 2013). Our results show that CRHR1 endocytosis contributes to the overall cAMP response, in line with the emerging paradigm of endosomal generation of cAMP by GPCRs, the mechanisms of which are just beginning to be understood. For the prototypical class A GPCR β-adrenergic receptor 2, the existence of a second phase of Gs coupling from endosomes has been elegantly shown (Irannejad et al., 2013), whereas for the class B PTHR,

Published July 11, 2016

a prolonged Gs coupling favored by ERK1/2 and β-arrestin was demonstrated (Feinstein et al., 2011).

Our present findings reveal a Gs-independent mechanism of cAMP production with an essential role in ligand-activated GPCR endocytosis-mediated signaling. Although there is no doubt that CRHR1 activates G protein–responsive tmACs at the plasma membrane (Punn et al., 2012), our data support a critical contribution of G protein–independent sAC to the cAMP response to CRH that is linked to ERK1/2 activation in cellular contexts of CRHR1 signaling.

Notably, most sustained cAMP responses have been reported for class B GPCRs that mediate the functions of therapeutically relevant peptide hormones (Ferrandon et al., 2009; Feinstein et al., 2013; Kuna et al., 2013; Merriam et al., 2013). Future work needs to focus on defining factors that modulate kinetics and spatial organization of the CRHR1-mediated cAMP response, which is thought to have significant physiological implications (Feinstein et al., 2011; Tsvetanova and von Zastrow, 2014). Furthermore, understanding the role of G protein– and endosome-dependent signaling, together with the identification of ligands with functional selectivity, may result in clinically valuable tools for pathologies involving the CRH/CRHR1 system.

Materials and methods

Cell culture and transfection

HT22-CRHR1, AtT20, and 3T3-L1-CRHR1 cell lines were cultured in DMEM supplemented with FBS (5% for HT22-CRHR1 and 10% for AtT20 and 3T3-L1-CRHR1), 2 mM L-glutamine, 100 U/ml penicillin, and 100 µg/ml streptomycin (Invitrogen) at 37°C in a humidified atmosphere containing 5% CO_2.

Plasmids were transfected using Lipofectamine and Plus Reagent (Invitrogen) according to the manufacturer's instructions and as previously described (Bonfiglio et al., 2013). Experiments were performed 48 h after plasmid transfection. When single-cell measurements were performed in cells transiently transfected with plasmids, cells were cotransfected with a fluorescent protein–expressing plasmid, and only fluorescent cells were used for the studies. siRNA transfection with Lipofectamine 2000 (Invitrogen) was performed as previously described (Bonfiglio et al., 2013) and according to the manufacturer's protocol. Experiments were performed 72 h after siRNA transfection. The efficiency of knockdown was assessed by quantitative RT-PCR normalized to HPRT, and experiments with at least 65% reduction of mRNA levels were considered.

Plasmids and siRNA

Plasmids were provided as follows: the mouse CRHR1 expression vectors c-Myc-mCRHR1 and myc-GFP-CRHR1 by J. Deussing (Max Planck Institute of Psychiatry, Munich, Germany); mTurquoise2-EPAC-cp173Venus-Venus (Epac-S^{H187}) by K. Jalink (Netherlands Cancer Institute, Amsterdam, Netherlands); AKAR4 by J. Zhang (Johns Hopkins University, Baltimore, MD); REX-GECO1 by R. Campbell (University of Alberta, Edmonton, AB, Canada); the dynamin-K44A expression vector by J. Benovic (Thomas Jefferson University, Philadelphia, PA); mCherry by M. Rossi (Instituto de Investigación en Biomedicina de Buenos Aires, Buenos Aires, Argentina); and EPAC1 and N-EPAC by D.L. Altschuler (University of Pittsburgh School of Medicine, Pittsburgh, PA).

Rat sACfl plasmid was obtained from Addgene (pSAC5.02, plasmid #16077). A truncated, catalytically active form of sAC (sACt; Tresguerres et al., 2011) tagged with the epitope HA at the C terminus was generated by PCR (sACt-HA). The first 468 aa were amplified via PCR from sACfl using ApaI and NotI restriction sites for N and C termini, respectively, and with the C terminus of sACt and the sequence of the epitope (YPYDVPDYA) encoded in the reverse primer. The insert was ligated into pcDNA3.1(+)/Zeo (Invitrogen).

sAC knockdown was achieved using a 21-nucleotide siRNA (5′-AAUGUAUGGGCUUCAUGGAtt-3′). siRNAs against AC1 and AC8 were purchased from GE Healthcare as pools of four siRNAs (SMART pools; Thermo Fisher Scientific). For EPAC knockdown, the following siRNAs were used: EPAC1 (5′-GGUCAAUUCUGCCGGUGAUtt-3′ and 5′-CGACACCACAGGUUGGAAAtt-3′) and EPAC2 (5′-GCUGGUAGACUGGAUGAUAtt-3′ and 5′-GCUAAUCUACCACACAUUUtt-3′). An siRNA against GL3 (5′-CUUACGCUGAGUACUUCGATT-3′) was used as control.

Generation of stable cell lines

HT22 stable clones expressing cMyc-CRHR1 were previously described (Bonfiglio et al., 2013). Stable clones expressing both cMyc-CRHR1 and FRET biosensors (Epac-S^{H187} or AKAR4) were obtained by transfection of HT22-CRHR1 cells with pcDNA3.1/Zeo(+)-Epac-S^{H187} or pcDNA3.1/Zeo(+)-AKAR4 and selection with Zeocin (100 µg/ml; Invitrogen). 3T3-L1 stable clones expressing cMyc-CRHR1 were obtained by transfection of pcDNA3-c-Myc-mCRHR1 and selection with Geneticin (800 µg/ml). In both cases, after 14 d of antibiotic treatment, clonal colonies were isolated and subcultured.

RT-PCR and quantitative real-time PCR

Total RNA was extracted from cell lines or total mouse brain extracts using TRI reagent (MRC), and complementary DNA synthesis was performed using M-MLV reverse transcription in the presence of RNasin RNase inhibitor (Promega). PCR primers were all intron spanning. cDNAs were amplified using Taq DNA polymerase (Invitrogen). Quantitative real-time PCR was performed with SYBR Green I (Roche) using a CFX96 Touch Real-Time PCR Detection System. Relative expression was calculated for each gene by the Ct method with HPRT for normalization.

Sequences and expected product sizes are as follows: sAC sense 5′-CCTGCATCGCTGTCTGGTAT-3′, antisense 5′-GAACTGTCGGGGTTCTTCGT-3′ (102 bp); AC1 sense 5′-GTGGCCAGTCGGATGGATAG-3′, antisense 5′-TTCACGCTGACTTTGCCTCT-3′ (119 bp); AC8 sense 5′-ACGTCATCATCTTCGCTTCCA-3′, antisense 5′-AGTACTCTGGGTAGGAGCAGA-3′ (150 bp); EPAC1 sense 5′-TCTTACCAGCTAGTGTTCGAGC-3′, antisense 5′-AATGCCGATATAGTCGCAGATG-3′ (223 bp); EPAC2 sense 5′-TAAAAGGCCGTTGGAGCGAT-3′, antisense 5′-GCCAGGACAGCATACCAGTT-3′ (195 bp); HPRT sense 5′-TGGGCTTACCTCACTGCTTTCC-3′, antisense 5′-CCTGGTTCATCATCGCTAATCACG-3′ (139 bp); and β-actin sense 5′-TGACGGGGTCACCCACACTGTGCCCATCTA-3′, antisense 5′-CTAGAAGCATTTGCGGTGGACGATGGAGGG-3′ (663 bp).

Ligand stimulation, drugs, and pharmacological inhibitors

For MAPK assays, cells were serum-starved for 6 h in OptiMEM before drug pretreatments or stimulation. Cells were stimulated with human/rat CRH (H-2435; Bachem), forskolin (13019; Cayman Chemical), and 8-CPT-cAMP (F1221, Sigma-Aldrich) at the concentrations and time points indicated. After incubation, cells were washed with ice-cold PBS and maintained in ice. When calcium chelators BAPTA-AM (B6769; Thermo Fisher Scientific), EGTA (E3889; Sigma-Aldrich), or pharmacologic inhibitors were used, cells were pretreated with the drugs or vehicle 15–30 min before stimulation. The following inhibitors were used: KT5720 (PKA; K3761; Sigma-Aldrich), RpcAMPS

Published July 11, 2016

(PKA; 1337; Tocris Bioscience), ddA (tmACs; 288104; EMD Millipore), KH7 (sAC; 3834; Tocris Bioscience), 2-HE (sAC; 13019; Cayman Chemical), DIDS, anion channel blocker (D3514; Sigma-Aldrich), U0126 (MEK; 662005; EMD Millipore), ESI09 (EPAC1/2; SML0814; Sigma-Aldrich), and Dyngo-4a (dynamin; ab120689; Abcam).

For experiments testing bicarbonate dependence, bicarbonate-free DMEM supplemented with 25 mM Hepes was used to prepare media at 0- and 25-mM sodium bicarbonate concentrations. Each condition was adjusted to physiological pH 7.2 with NaOH and HCl and allowed to equilibrate in the incubator for additional 30 min, and then the pH was checked again and adjusted to 7.4. HT22-CRHR1 cells were serum-starved for 6 h in bicarbonate-free DMEM or 25 mM bicarbonate DMEM before stimulation with 10 nM CRH.

Preparation of cellular extracts and immunoblotting

After treatments, cells were washed with ice-cold PBS and lysed in Laemmli sample buffer. Whole-cell lysates were sonicated and heated to 95°C for 5 min. Samples were resolved by SDS-PAGE and transferred to 0.45-mm nitrocellulose membranes (EMD Millipore) for immunoblotting. Membranes were blocked in TBS–Tween 20 (0.05%) containing 5% milk at RT for 1 h under shaking and probed overnight at 4°C with the primary antibodies. The following antibodies were used: anti-sAC (R21; CEP Biotech), anti–c-Myc (9E10; sc-40) and anti–pERK1/2 (E-4; sc-7383) from Santa Cruz Biotechnology, Inc.; anti–total-ERK1/2 (9102; Cell Signaling Technology), anti-phospho CREB (06-519; EMD Millipore), and anti–total-CREB (9104; Cell Signaling Technology).

Chemiluminescent signals were detected by HRP-conjugated secondary antibodies and enhanced chemiluminescence (SuperSignal West Dura; Thermo Fisher Scientific) using a GBOX Chemi XT4 (Syngene). Phosphorylation of MAPK and CREB was detected with the Odyssey Fc Imaging System (LI-COR Biosciences), using anti-mouse-IRDye700DX and anti-rabbit-IRDye800CW secondary antibodies (Rockland). Phosphorylated proteins were relativized to the total protein level, and results were expressed as the percentage of maximum pERK1/2 after stimulation. Immunoreactive signals were analyzed digitally using ImageJ software (National Institutes of Health).

Neurite outgrowth assay

HT22-CRHR1 cells seeded at 40% density in 12-well plates were stimulated with 100 nM CRH in the presence of vehicle or tmAC- or sAC-specific inhibitors. After 20 h of treatment, cells were imaged under bright-field illumination using an Olympus IX81 inverted epifluorescence microscope with a 20× air objective and Metamorph software for image acquisition. For each treatment, at least 15 random fields were imaged. Quantification of morphological changes was performed using Simple Neurite Tracer plugin for Fiji software. Neurite outgrowth was determined as the ratio between the longest neurite and the soma diameter per cell after 20 h, measuring at least 100 cells per treatment. For statistical analysis, repeated-measures one-way analysis of variance followed by Tukey's post hoc test ($n = 3$) was performed.

Single-cell intracellular calcium imaging

For experiments using ester calcium indicators, cells plated in glass-bottom dishes were loaded for 30–60 min in darkness with 6 µM Fluo-4-AM and 0.14% Pluronic F-127 (Molecular Probes) in Ringer buffer. Images were acquired with a Axio Observer Z1 inverted Epifluorescence microscope (ZEISS), equipped with an AxioCam HRm3 digital CCD camera, a Stage Controller XY STEP SMC 2009 scanning stage, and an Incubator XLmulti S1 (D) and Heating Unit XL S1 (D) for live-imaging incubation. Data acquisition was controlled by Zen Blue 2011 software (ZEISS), configured at a bit depth of 14 bits. Cells were imaged with a 20× air objective (Plan-Apochromat NA 0.8 M27) and illuminated using Colibri.2 470-nm LED excitation (5% power), with a 50-ms exposure acquired every 5 s and a 38HE Filter set for a duration of 10 min. When indicated, cells were preincubated with different reagents. Approximately 30 s after the start of the experiment, CRH was added to a final concentration of 100 nM. Image analysis was performed with Fiji by measuring calcium-dependent changes in fluorescence intensity from resting levels ($\Delta F/F_0$) in 30–40 cells randomly selected in each experiment.

Spectral FRET and coimaging of cAMP and calcium

HT22-CRHR1, AtT20, or 3T3-CRHR1 cells expressing fluorescent proteins and FRET biosensors were seeded in glass-bottom dishes. Cell imaging was performed on an inverted LSM 710 (ZEISS) equipped with an automated stage, an incubation chamber, and Definite focus system. Data acquisition was performed with ZEN Black 2011 software**.** Images were acquired with a C-Apochromat 40×/1.2 water immersion and temperature-corrected objective lens at 1,024 × 1,024 pixels, 16 bits, pixel dwell time 3.15 µs, with open pinhole (600 µm). The emission spectra of the fluorescent proteins Cerulean, mTurquoise2, Venus, and REX-GECO1 bound to calcium were determined using 405- or 458-nm lasers for the excitation and lambda mode for the detection using a 32-channel QUASAR detector arranged with bandwidth channels of 9.7 nm.

For FRET experiments, cells were illuminated with a 30-mW, 405-nm diode laser at 2% laser power (550–650 gain) and a 405-nm dichroic mirror; emission was collected at 413- to 723-nm wavelengths every 15 s for a duration of 15 min. For coimaging cAMP and calcium dynamics, a 25-mW argon laser for 458-nm excitation (2.5% power, 650 gain) and a 458-nm dichroic mirror were used; emission was collected at 463- to 723-nm wavelengths every 5 s for a duration of 10 min. The saturation level was verified for each image.

For the reference spectra and the experiments, phenol red–free DMEM/F12 medium supplemented with 20 mM Hepes was used, and imaging was performed at 37°C and 5% CO_2. Approximately 2.5 min after the start of the experiment, CRH was added to the final concentration indicated. When indicated, cells were preincubated for 15 min with different reagents. AC inhibitors were also added after CRH stimulation to evaluate the change in the FRET time course.

For lambda FRET experiments, the linear unmixing tool of ZEN Black 2011 software was used to obtain an image for each fluorophore using the reference spectra. Image quantification was performed with Fiji software. After background subtraction, REX-GECO1, FRET, and donor intensities were measured for single cells for each time point. The FRET/donor ratio or REX-GECO1 intensity was calculated and normalized to resting levels (before stimulation).

Flow cytometry assays

For CRHR1 surface staining, HT22-CRHR1 cells on 60-mm plates were starved for 1 h in OptiMEM before drug pretreatments or stimulation. When pharmacological inhibitors were used, cells were pretreated with drugs or vehicle 15–30 min before stimulation with CRH for the indicated concentration and time. After incubation, cells were washed with ice-cold PBS and harvested in 1 mM PBS-EDTA. 2.0×10^5 cells were incubated at 4 C with 10% FBS in PBS for 1 h to reduce nonspecific binding. Subsequently, cells were incubated with 0.2 µg anti–c-Myc monoclonal antibody (Santa Cruz Biotechnology, Inc.) for 2 h and, after washing with 1% FBS in PBS, were stained with 1.4 µg anti-mouse Alexa Fluor 647–conjugated secondary antibody (Thermo Fisher Scientific). All solutions contained 0.01% sodium azide. Controls for autofluorescence, primary antibody staining on parental HT22 cells, and secondary antibody staining in absence of primary

Published July 11, 2016

antibody were performed for each experiment. Flow cytometry data were acquired on a FACsCANTO II (BD). Data were analyzed using FlowJo software (Tree Star).

Confocal microscopy

HT22-CRHR1 cells transiently transfected with cMyc-GFP-CRHR1 expression vector were seeded on glass coverslips. After treatment, cells were washed with ice-cold PBS, fixed with 4% paraformaldehyde in PBS, permeabilized with 0.01% Triton X-100/PBS, and stained with DAPI. Coverslips were washed with PBS, and cells were mounted with Mowiol and analyzed by confocal microscopy. Images were acquired on an inverted LSM 710. Data acquisition was performed with ZEN Black 2011 software. Images were acquired with a C-Apochromat 63×/1.2 water immersion and temperature-corrected objective lens at 1,024 × 1,024 pixels, 12 bits, pixel dwell time 0.52 µs, with 1 Airy unit. For each treatment, 15–20 individual cells were randomly selected and examined. No fluorescence was observed for control cells transfected with an empty vector.

Competition cAMP binding assay

cAMP determination by means of competition with [^{3}H]cAMP for PKA was performed as previously described (Copsel et al., 2011; Bonfiglio et al., 2013). In brief, HT22-CRHR1 cells were pretreated for 30 min with the indicated inhibitors, stimulated with CRH, and subjected to ethanol extraction followed by 15-min centrifugation at 3,000 *g*. Supernatants were dried and resuspended in 50 mM Tris-HCl buffer, pH 7.4. cAMP content was determined by means of competition with [^{3}H]cAMP for PKA and expressed as the percentage of stimulation relative to maximum response. The standard curve was performed using eight cAMP amounts ranging from 0.1 to 90 pmol. Duplicate samples in at least three independent experiments were analyzed.

Pomc–Luc reporter assay

Luciferase reporter assays were performed as previously described (Riebold et al., 2015). In brief, AtT-20 cells were seeded in 48-well plates and transfected with 0.3 µg *Pomc*–Luc and 0.1 µg RSV-Gal (Addgene) for normalization for 3 h using Superfect (QIAGEN) according to the manufacturer's instructions. Transfection mix was replaced with serum-free culture medium overnight. 24 h after transfection, cells were pretreated with vehicle or sAC-specific inhibitors and stimulated with 100 nM CRH for 6 h. Cells were lysed in Passive Lysis Buffer (Promega), followed by measurement of reporter activity according to the manufacturer's instructions (PJK GmbH). Relative Luc values (Luc/β-Gal) were used to normalize for transfection efficiency in all experiments.

Statistics

Each experiment was performed at least three independent times. The results are presented as the mean ± SEM of each measurement. Comparisons between treatments were performed using Student's *t* test and one- or two-way analysis of variance (GraphPad Prism) followed by post hoc Tukey's test. Statistically significant differences are indicated.

Online supplemental material

Fig. S1 shows the optimization of cAMP measurements by FRET, CRH-triggered cAMP response by competition with [^{3}H]cAMP for PKA, sAC detection by Western blot, and effect of sAC-specific inhibitors in CRH-mediated ERK1/2 activation. Fig. S2 shows cAMP and ERK1/2 responses triggered by CRH and PACAP38 in AtT20 cells, ERK1/2 and CREB activation, and calcium response to CRH in 3T3L1-CRHR1 cells. Fig. S3 shows CRH-dependent CRHR1 endocytosis blocked by DynK44A and Dyngo-4a, calcium response to CRH when endocytosis is blocked, cAMP and ERK1/2 response in the presence of MEK1/2 inhibitors, and sustained cAMP response in the presence and absence of ddA. Fig. S4 demonstrates the role of calcium in ERK1/2 activation in response to CRH and the expression of AC8 in HT22-CRHR1 cells. Online supplemental material is available at http://www.jcb.org/cgi/content/full/jcb.201512075/DC1.

Acknowledgments

We thank E. Arzt for providing intellectual input and critical advice for experimental development and data interpretation, M. Páez-Pereda for advice on *Pomc*–Luc experiments, C. Davio for contributing expertise and reagents for experiments of binding assay for cAMP determination, A. Bruzzone and I.A. Lüthy for providing isoproterenol, and A. Attorresi and C. Pollack for excellent technical assistance with microscopy and flow cytometry experiments.

This work was supported by grants from the Agencia Nacional de Promoción Científica y Tecnológica (Max-Planck 10:2791 and 13:0392) to S. Silberstein and C.W. Turck, the Max Planck Society, the University of Buenos Aires, the Consejo Nacional de Investigaciones Científicas y Técnicas, and the Fondo para la Convergencia Estructural del Mercosur (COF 03/11).

The authors declare no competing financial interests.

Submitted: 23 December 2015
Accepted: 10 June 2016

References

Allen, M.D., and J. Zhang. 2006. Subcellular dynamics of protein kinase A activity visualized by FRET-based reporters. *Biochem. Biophys. Res. Commun.* 348:716–721. http://dx.doi.org/10.1016/j.bbrc.2006.07.136

Appukuttan, A., J.P. Flacke, H. Flacke, A. Posadowsky, H.P. Reusch, and Y. Ladilov. 2014. Inhibition of soluble adenylyl cyclase increases the radiosensitivity of prostate cancer cells. *Biochim. Biophys. Acta.* 1842(12, 12 Pt B):2656–2663. http://dx.doi.org/10.1016/j.bbadis.2014.09.008

Bitterman, J.L., L. Ramos-Espiritu, A. Diaz, L.R. Levin, and J. Buck. 2013. Pharmacological distinction between soluble and transmembrane adenylyl cyclases. *J. Pharmacol. Exp. Ther.* 347:589–598. http://dx.doi.org/10.1124/jpet.113.208496

Bonfiglio, J.J., C. Inda, D. Refojo, F. Holsboer, E. Arzt, and S. Silberstein. 2011. The corticotropin-releasing hormone network and the hypothalamic-pituitary-adrenal axis: Molecular and cellular mechanisms involved. *Neuroendocrinology.* 94:12–20. http://dx.doi.org/10.1159/000328226

Bonfiglio, J.J., C. Inda, S. Senin, G. Maccarrone, D. Refojo, D. Giacomini, C.W. Turck, F. Holsboer, E. Arzt, and S. Silberstein. 2013. B-Raf and CRHR1 internalization mediate biphasic ERK1/2 activation by CRH in hippocampal HT22 cells. *Mol. Endocrinol.* 27:491–510. http://dx.doi.org/10.1210/me.2012-1359

Carlson, A.E., B. Hille, and D.F. Babcock. 2007. External Ca2+ acts upstream of adenylyl cyclase SACY in the bicarbonate signaled activation of sperm motility. *Dev. Biol.* 312:183–192. http://dx.doi.org/10.1016/j.ydbio.2007.09.017

Chen, Y., M.J. Cann, T.N. Litvin, V. Iourgenko, M.L. Sinclair, L.R. Levin, and J. Buck. 2000. Soluble adenylyl cyclase as an evolutionarily conserved bicarbonate sensor. *Science.* 289:625–628 http://dx.doi.org/. http://dx.doi.org/10.1126/science.289.5479.625

Choi, H.B., G.R. Gordon, N. Zhou, C. Tai, R.L. Rungta, J. Martinez, T.A. Milner, J.K. Ryu, J.G. McLarnon, M. Tresguerres, et al. 2012. Metabolic communication between astrocytes and neurons via bicarbonate-responsive soluble adenylyl cyclase. *Neuron.* 75:1094–1104. http://dx.doi.org/10.1016/j.neuron.2012.08.032

Copsel, S., C. Garcia, F. Diez, M. Vermeulem, A. Baldi, L.G. Bianciotti, F.G. Russel, C. Shayo, and C. Davio. 2011. Multidrug resistance protein 4 (MRP4/ABCC4) regulates cAMP cellular levels and controls human leukemia cell proliferation and differentiation. *J. Biol. Chem.* 286:6979–6988. http://dx.doi.org/10.1074/jbc.M110.166868

Corredor, R.G., E.F. Trakhtenberg, W. Pita-Thomas, X. Jin, Y. Hu, and J.L. Goldberg. 2012. Soluble adenylyl cyclase activity is necessary for retinal ganglion cell survival and axon growth. *J. Neurosci.* 32:7734–7744. http://dx.doi.org/10.1523/JNEUROSCI.5288-11.2012

Depry, C., M.D. Allen, and J. Zhang. 2011. Visualization of PKA activity in plasma membrane microdomains. *Mol. Biosyst.* 7:52–58. http://dx.doi.org/10.1039/C0MB00079E

Feinstein, T.N., V.L. Wehbi, J.A. Ardura, D.S. Wheeler, S. Ferrandon, T.J. Gardella, and J.P. Vilardaga. 2011. Retromer terminates the generation of cAMP by internalized PTH receptors. *Nat. Chem. Biol.* 7:278–284. http://dx.doi.org/10.1038/nchembio.545

Feinstein, T.N., N. Yui, M.J. Webber, V.L. Wehbi, H.P. Stevenson, J.D. King Jr., K.R. Hallows, D. Brown, R. Bouley, and J.P. Vilardaga. 2013. Noncanonical control of vasopressin receptor type 2 signaling by retromer and arrestin. *J. Biol. Chem.* 288:27849–27860. http://dx.doi.org/10.1074/jbc.M112.445098

Ferrandon, S., T.N. Feinstein, M. Castro, B. Wang, R. Bouley, J.T. Potts, T.J. Gardella, and J.P. Vilardaga. 2009. Sustained cyclic AMP production by parathyroid hormone receptor endocytosis. *Nat. Chem. Biol.* 5:734–742. http://dx.doi.org/10.1038/nchembio.206

Flacke, J.P., H. Flacke, A. Appukuttan, R.J. Palisaar, J. Noldus, B.D. Robinson, H.P. Reusch, J.H. Zippin, and Y. Ladilov. 2013. Type 10 soluble adenylyl cyclase is overexpressed in prostate carcinoma and controls proliferation of prostate cancer cells. *J. Biol. Chem.* 288:3126–3135. http://dx.doi.org/10.1074/jbc.M112.403279

Gutknecht, E., I. Van der Linden, K. Van Kolen, K.F. Verhoeven, G. Vauquelin, and F.M. Dautzenberg. 2009. Molecular mechanisms of corticotropin-releasing factor receptor-induced calcium signaling. *Mol. Pharmacol.* 75:648–657. http://dx.doi.org/10.1124/mol.108.050427

Halm, S.T., J. Zhang, and D.R. Halm. 2010. beta-Adrenergic activation of electrogenic K+ and Cl- secretion in guinea pig distal colonic epithelium proceeds via separate cAMP signaling pathways. *Am. J. Physiol. Gastrointest. Liver Physiol.* 299:G81–G95. http://dx.doi.org/10.1152/ajpgi.00035.2010

Han, H., A. Stessin, J. Roberts, K. Hess, N. Gautam, M. Kamenetsky, O. Lou, E. Hyde, N. Nathan, W.A. Muller, et al. 2005. Calcium-sensing soluble adenylyl cyclase mediates TNF signal transduction in human neutrophils. *J. Exp. Med.* 202:353–361. http://dx.doi.org/10.1084/jem.20050778

Hess, K.C., B.H. Jones, B. Marquez, Y. Chen, T.S. Ord, M. Kamenetsky, C. Miyamoto, J.H. Zippin, G.S. Kopf, S.S. Suarez, et al. 2005. The "soluble" adenylyl cyclase in sperm mediates multiple signaling events required for fertilization. *Dev. Cell.* 9:249–259. http://dx.doi.org/10.1016/j.devcel.2005.06.007

Holmes, K.D., A.V. Babwah, L.B. Dale, M.O. Poulter, and S.S. Ferguson. 2006. Differential regulation of corticotropin releasing factor 1alpha receptor endocytosis and trafficking by beta-arrestins and Rab GTPases. *J. Neurochem.* 96:934–949. http://dx.doi.org/10.1111/j.1471-4159.2005.03603.x

Holsboer, F., and M. Ising. 2010. Stress hormone regulation: Biological role and translation into therapy. *Annu. Rev. Psychol.* 61:81–109: C1–C11. http://dx.doi.org/10.1146/annurev.psych.093008.100321

Irannejad, R., and M. von Zastrow. 2014. GPCR signaling along the endocytic pathway. *Curr. Opin. Cell Biol.* 27:109–116. http://dx.doi.org/10.1016/j.ceb.2013.10.003

Irannejad, R., J.C. Tomshine, J.R. Tomshine, M. Chevalier, J.P. Mahoney, J. Steyaert, S.G. Rasmussen, R.K. Sunahara, H. El-Samad, B. Huang, and M. von Zastrow. 2013. Conformational biosensors reveal GPCR signalling from endosomes. *Nature.* 495:534–538. http://dx.doi.org/10.1038/nature12000

Ivonnet, P., M. Salathe, and G.E. Conner. 2015. Hydrogen peroxide stimulation of CFTR reveals an Epac-mediated, soluble AC-dependent cAMP amplification pathway common to GPCR signalling. *Br. J. Pharmacol.* 172:173–184. http://dx.doi.org/10.1111/bph.12934

Jaiswal, B.S., and M. Conti. 2003. Calcium regulation of the soluble adenylyl cyclase expressed in mammalian spermatozoa. *Proc. Natl. Acad. Sci. USA.* 100:10676–10681. http://dx.doi.org/10.1073/pnas.1831008100

Kawasaki, H., G.M. Springett, N. Mochizuki, S. Toki, M. Nakaya, M. Matsuda, D.E. Housman, and A.M. Graybiel. 1998. A family of cAMP-binding proteins that directly activate Rap1. *Science.* 282:2275–2279 http://dx.doi.org/. http://dx.doi.org/10.1126/science.282.5397.2275

Klarenbeek, J., J. Goedhart, A. van Batenburg, D. Groenewald, and K. Jalink. 2015. Fourth-generation epac-based FRET sensors for cAMP feature exceptional brightness, photostability and dynamic range: characterization of dedicated sensors for FLIM, for ratiometry and with high affinity. *PLoS One.* 10:e0122513. http://dx.doi.org/10.1371/journal.pone.0122513

Kleinboelting, S., A. Diaz, S. Moniot, J. van den Heuvel, M. Weyand, L.R. Levin, J. Buck, and C. Steegborn. 2014. Crystal structures of human soluble adenylyl cyclase reveal mechanisms of catalysis and of its activation through bicarbonate. *Proc. Natl. Acad. Sci. USA.* 111:3727–3732. http://dx.doi.org/10.1073/pnas.1322778111

Kotowski, S.J., F.W. Hopf, T. Seif, A. Bonci, and M. von Zastrow. 2011. Endocytosis promotes rapid dopaminergic signaling. *Neuron.* 71:278–290. http://dx.doi.org/10.1016/j.neuron.2011.05.036

Kovalovsky, D., D. Refojo, A.C. Liberman, D. Hochbaum, M.P. Pereda, O.A. Coso, G.K. Stalla, F. Holsboer, and E. Arzt. 2002. Activation and induction of NUR77/NURR1 in corticotrophs by CRH/cAMP: Involvement of calcium, protein kinase A, and MAPK pathways. *Mol. Endocrinol.* 16:1638–1651 http://dx.doi.org/. http://dx.doi.org/10.1210/mend.16.7.0863

Kuna, R.S., S.B. Girada, S. Asalla, J. Vallentyne, S. Maddika, J.T. Patterson, D.L. Smiley, R.D. DiMarchi, and P. Mitra. 2013. Glucagon-like peptide-1 receptor-mediated endosomal cAMP generation promotes glucose-stimulated insulin secretion in pancreatic β-cells. *Am. J. Physiol. Endocrinol. Metab.* 305:E161–E170. http://dx.doi.org/10.1152/ajpendo.00551.2012

Lefkimmiatis, K., D. Leronni, and A.M. Hofer. 2013. The inner and outer compartments of mitochondria are sites of distinct cAMP/PKA signaling dynamics. *J. Cell Biol.* 202:453–462. http://dx.doi.org/10.1083/jcb.201303159

Litvin, T.N., M. Kamenetsky, A. Zarifyan, J. Buck, and L.R. Levin. 2003. Kinetic properties of "soluble" adenylyl cyclase. Synergism between calcium and bicarbonate. *J. Biol. Chem.* 278:15922–15926. http://dx.doi.org/10.1074/jbc.M212475200

Liu, B., G.D. Hammer, M. Rubinstein, M. Mortrud, and M.J. Low. 1992. Identification of DNA elements cooperatively activating proopiomelanocortin gene expression in the pituitary glands of transgenic mice. *Mol. Cell. Biol.* 12:3978–3990 http://dx.doi.org/. http://dx.doi.org/10.1128/MCB.12.9.3978

Lohse, M.J., and D. Calebiro. 2013. Cell biology: Receptor signals come in waves. *Nature.* 495:457–458. http://dx.doi.org/10.1038/nature12086

Merriam, L.A., C.N. Baran, B.M. Girard, J.C. Hardwick, V. May, and R.L. Parsons. 2013. Pituitary adenylate cyclase 1 receptor internalization and endosomal signaling mediate the pituitary adenylate cyclase activating polypeptide-induced increase in guinea pig cardiac neuron excitability. *J. Neurosci.* 33:4614–4622. http://dx.doi.org/10.1523/JNEUROSCI.4999-12.2013

Oakley, R.H., J.A. Olivares-Reyes, C.C. Hudson, F. Flores-Vega, F.M. Dautzenberg, and R.L. Hauger. 2007. Carboxyl-terminal and intracellular loop sites for CRF1 receptor phosphorylation and beta-arrestin-2 recruitment: A mechanism regulating stress and anxiety responses. *Am. J. Physiol. Regul. Integr. Comp. Physiol.* 293:R209–R222. http://dx.doi.org/10.1152/ajpregu.00099.2006

Onodera, Y., J.M. Nam, and M.J. Bissell. 2014. Increased sugar uptake promotes oncogenesis via EPAC/RAP1 and O-GlcNAc pathways. *J. Clin. Invest.* 124:367–384. http://dx.doi.org/10.1172/JCI63146

Peeters, P.J., H.W. Göhlmann, I. Van den Wyngaert, S.M. Swagemakers, L. Bijnens, S.U. Kass, and T. Steckler. 2004. Transcriptional response to corticotropin-releasing factor in AtT-20 cells. *Mol. Pharmacol.* 66:1083–1092. http://dx.doi.org/10.1124/mol.104.000950

Perry, S.J., S. Junger, T.A. Kohout, S.R. Hoare, R.S. Struthers, D.E. Grigoriadis, and R.A. Maki. 2005. Distinct conformations of the corticotropin releasing factor type 1 receptor adopted following agonist and antagonist binding are differentially regulated. *J. Biol. Chem.* 280:11560–11568. http://dx.doi.org/10.1074/jbc.M412914200

Punn, A., J. Chen, M. Delidaki, J. Tang, G. Liapakis, H. Lehnert, M.A. Levine, and D.K. Grammatopoulos. 2012. Mapping structural determinants within third intracellular loop that direct signaling specificity of type 1 corticotropin-releasing hormone receptor. *J. Biol. Chem.* 287:8974–8985. http://dx.doi.org/10.1074/jbc.M111.272161

Rajagopal, S., K. Rajagopal, and R.J. Lefkowitz. 2010. Teaching old receptors new tricks: Biasing seven-transmembrane receptors. *Nat. Rev. Drug Discov.* 9:373–386. http://dx.doi.org/10.1038/nrd3024

Refojo, D., C. Echenique, M.B. Müller, J.M. Reul, J.M. Deussing, W. Wurst, I. Sillaber, M. Paez-Pereda, F. Holsboer, and E. Arzt. 2005. Corticotropin-releasing hormone activates ERK1/2 MAPK in specific brain areas. *Proc. Natl. Acad. Sci. USA.* 102:6183–6188. http://dx.doi.org/10.1073/pnas.0502070102

Rehmann, H. 2013. Epac-inhibitors: Facts and artefacts. *Sci. Rep.* 3:3032. http://dx.doi.org/10.1038/srep03032

Riebold, M., C. Kozany, L. Freiburger, M. Sattler, M. Buchfelder, F. Hausch, G.K. Stalla, and M. Paez-Pereda. 2015. A C-terminal HSP90 inhibitor restores glucocorticoid sensitivity and relieves a mouse allograft model of Cushing disease. *Nat. Med.* 21:276–280. http://dx.doi.org/10.1038/nm.3776

Shenoy, S.K., M.T. Drake, C.D. Nelson, D.A. Houtz, K. Xiao, S. Madabushi, E. Reiter, R.T. Premont, O. Lichtarge, and R.J. Lefkowitz. 2006. beta-Arrestin-dependent, G protein-independent ERK1/2 activation by the beta2 adrenergic receptor. *J. Biol. Chem.* 281:1261–1273. http://dx.doi.org/10.1074/jbc.M506576200

Steegborn, C., T.N. Litvin, L.R. Levin, J. Buck, and H. Wu. 2005. Bicarbonate activation of adenylyl cyclase via promotion of catalytic active site closure and metal recruitment. *Nat. Struct. Mol. Biol.* 12:32–37. http://dx.doi.org/10.1038/nsmb880

Tresguerres, M., L.R. Levin, and J. Buck. 2011. Intracellular cAMP signaling by soluble adenylyl cyclase. *Kidney Int.* 79:1277–1288. http://dx.doi.org/10.1038/ki.2011.95

Tsvetanova, N.G., and M. von Zastrow. 2014. Spatial encoding of cyclic AMP signaling specificity by GPCR endocytosis. *Nat. Chem. Biol.* 10:1061–1065. http://dx.doi.org/10.1038/nchembio.1665

Van Kolen, K., F.M. Dautzenberg, K. Verstraeten, I. Royaux, R. De Hoogt, E. Gutknecht, and P.J. Peeters. 2010. Corticotropin releasing factor-induced ERK phosphorylation in AtT20 cells occurs via a cAMP-dependent mechanism requiring EPAC2. *Neuropharmacology.* 58:135–144. http://dx.doi.org/10.1016/j.neuropharm.2009.06.022

Vilardaga, J.P., F.G. Jean-Alphonse, and T.J. Gardella. 2014. Endosomal generation of cAMP in GPCR signaling. *Nat. Chem. Biol.* 10:700–706. http://dx.doi.org/10.1038/nchembio.1611

Watson, R.L., J. Buck, L.R. Levin, R.C. Winger, J. Wang, H. Arase, and W.A. Muller. 2015. Endothelial CD99 signals through soluble adenylyl cyclase and PKA to regulate leukocyte transendothelial migration. *J. Exp. Med.* 212:1021–1041. http://dx.doi.org/10.1084/jem.20150354

Wertheimer, E., D. Krapf, J.L. de la Vega-Beltran, C. Sánchez-Cárdenas, F. Navarrete, D. Haddad, J. Escoffier, A.M. Salicioni, L.R. Levin, J. Buck, et al. 2013. Compartmentalization of distinct cAMP signaling pathways in mammalian sperm. *J. Biol. Chem.* 288:35307–35320. http://dx.doi.org/10.1074/jbc.M113.489476

Willoughby, D., and D.M. Cooper. 2007. Organization and Ca^{2+} regulation of adenylyl cyclases in cAMP microdomains. *Physiol. Rev.* 87:965–1010. http://dx.doi.org/10.1152/physrev.00049.2006

Wu, J., A.S. Abdelfattah, L.S. Miraucourt, E. Kutsarova, A. Ruangkittisakul, H. Zhou, K. Ballanyi, G. Wicks, M. Drobizhev, A. Rebane, et al. 2014. A long Stokes shift red fluorescent Ca2+ indicator protein for two-photon and ratiometric imaging. *Nat. Commun.* 5:5262. http://dx.doi.org/10.1038/ncomms6262

Wu, K.Y., J.H. Zippin, D.R. Huron, M. Kamenetsky, U. Hengst, J. Buck, L.R. Levin, and S.R. Jaffrey. 2006. Soluble adenylyl cyclase is required for netrin-1 signaling in nerve growth cones. *Nat. Neurosci.* 9:1257–1264. http://dx.doi.org/10.1038/nn1767

Zhu, Y., H. Chen, S. Boulton, F. Mei, N. Ye, G. Melacini, J. Zhou, and X. Cheng. 2015. Biochemical and pharmacological characterizations of ESI-09 based EPAC inhibitors: Defining the ESI-09 "therapeutic window". *Sci. Rep.* 5:9344. http://dx.doi.org/10.1038/srep09344

Zippin, J.H., J. Farrell, D. Huron, M. Kamenetsky, K.C. Hess, D.A. Fischman, L.R. Levin, and J. Buck. 2004. Bicarbonate-responsive "soluble" adenylyl cyclase defines a nuclear cAMP microdomain. *J. Cell Biol.* 164:527–534. http://dx.doi.org/10.1083/jcb.200311119

Inda et al., http://www.jcb.org/cgi/content/full/jcb.201512075/DC1

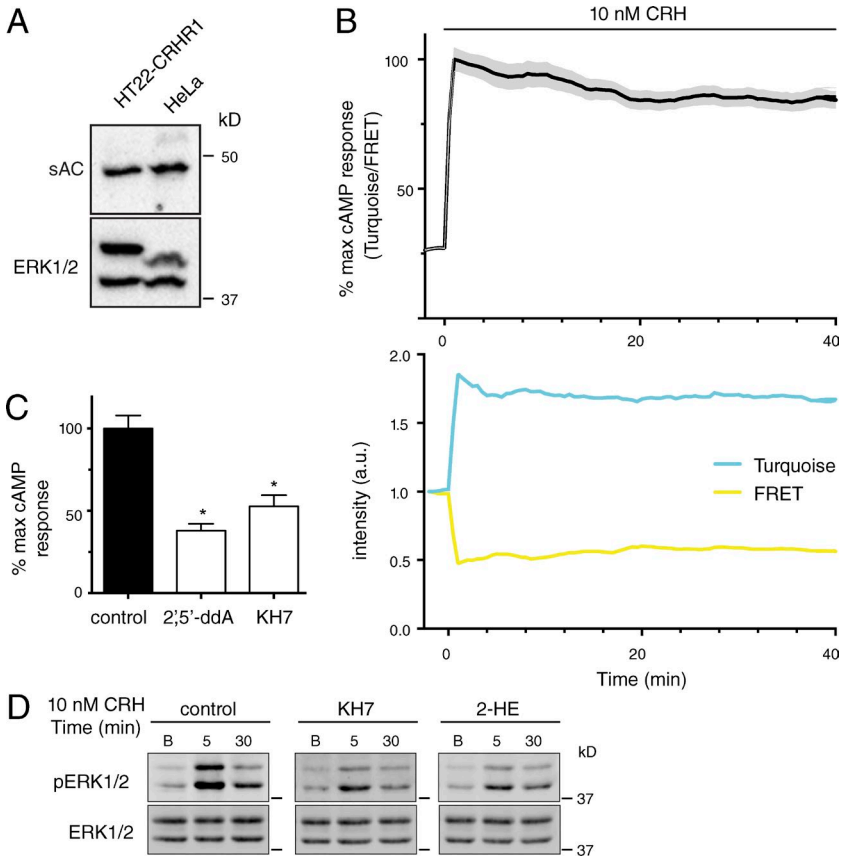

Figure S1. **Optimization of cAMP measurement in HT22-CRHR1 cells and sAC in the CRH response.** (A) By Western blot, a band of 48 kD was detected using a sAC monoclonal antibody (R21, CEP Biotech) in HT22-CRHR1 cell extracts. HeLa extracts were used as positive control, as indicated by the manufacturer, and ERK1/2 as a loading control. (B) HT22-CRHR1-Epac-S^{H187} cells were stimulated with CRH at time 0 (mean ± SEM, n = 16 cells). Time courses of the donor (mTurquoise2) and FRET mean intensity changes were determined relative to basal. a.u., arbitrary unit. (C) HT22-CRHR1 cells were preincubated with vehicle (control), tmAC inhibitor (50 µM ddA), or sAC inhibitor (7.5 µM KH7) and stimulated with 100 nM CRH. cAMP levels were determined by means of competition with [^{3}H]cAMP for PKA and expressed as the percentage of stimulation relative to maximal response (3 min after 100 nM CRH stimulation). Data are mean ± SEM, n = 3. *, $P < 0.05$ by one-way analysis of variance followed by Tukey's test. (D) pERK1/2 and total ERK1/2 were measured in HT22-CRHR1 cells preincubated with vehicle (control) or different sAC-specific inhibitors, KH7 (7.5 µM) or 2-HE (10 µM), and stimulated with CRH for the indicated times.

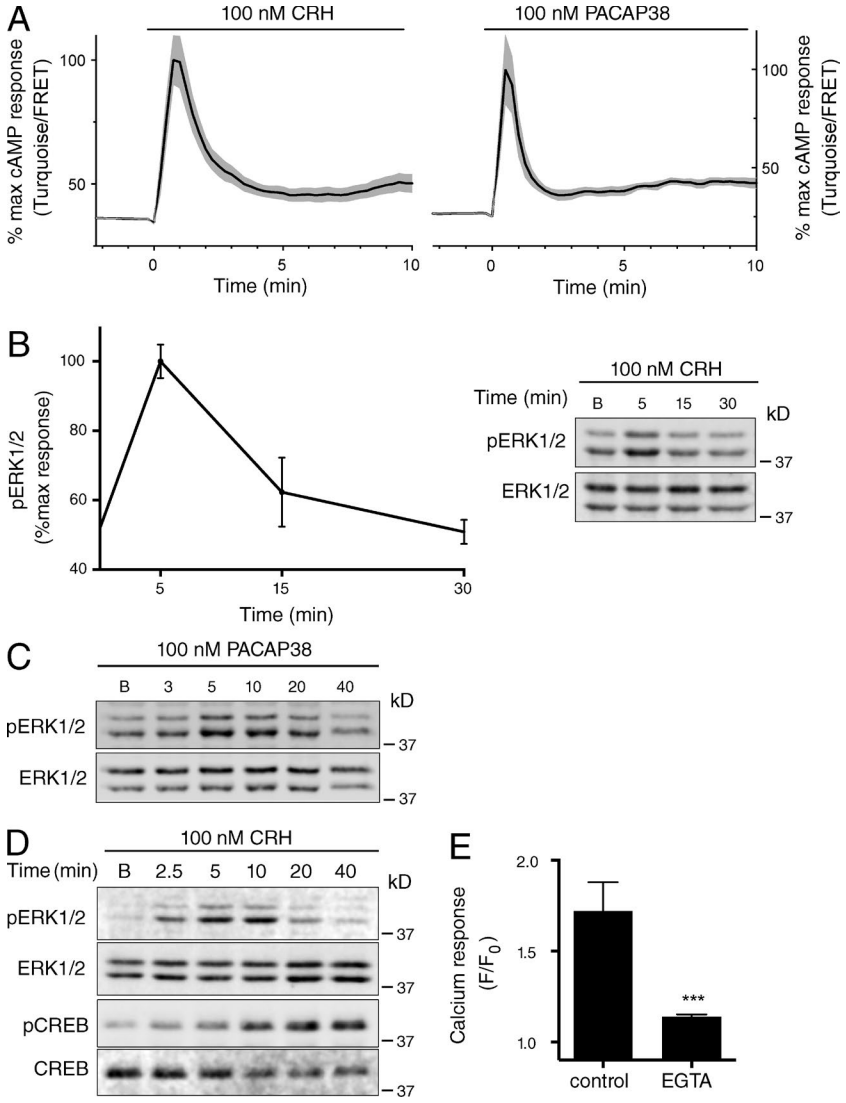

Figure S2. **CRH responses in AtT20 and 3T3L1-CRHR1 cell lines.** (A) AtT20 cells transiently transfected with the cAMP FRET-based biosensor Epac-S^{H187} were stimulated at time 0 with 100 nM CRH or 100 nM PACAP38. The time course of FRET changes was measured in single cells (mean ± SEM, 5 cells). (B and C) pERK1/2 and total ERK1/2 were measured in AtT20 cells stimulated with CRH or PACAP38 for the indicated times. (A) Signals were quantified, and each value of pERK1/2 was normalized to total ERK1/2. Results are expressed as the percentage of maximum pERK1/2 (mean ± SEM, $n = 3$). (D) pERK1/2, total ERK1/2, pCREB, and total CREB were measured in cell extracts of 3T3L1-CRHR1 cells stimulated with 100 nM CRH for the indicated times. (E) 3T3L1-CRHR1 cells were loaded with Fluo-4-AM and pretreated with 500 µM EGTA or vehicle. Calcium response was determined as fluorescence change 15 s after stimulation by 100 nM CRH. ***, $P < 0.001$ by Student's *t* test.

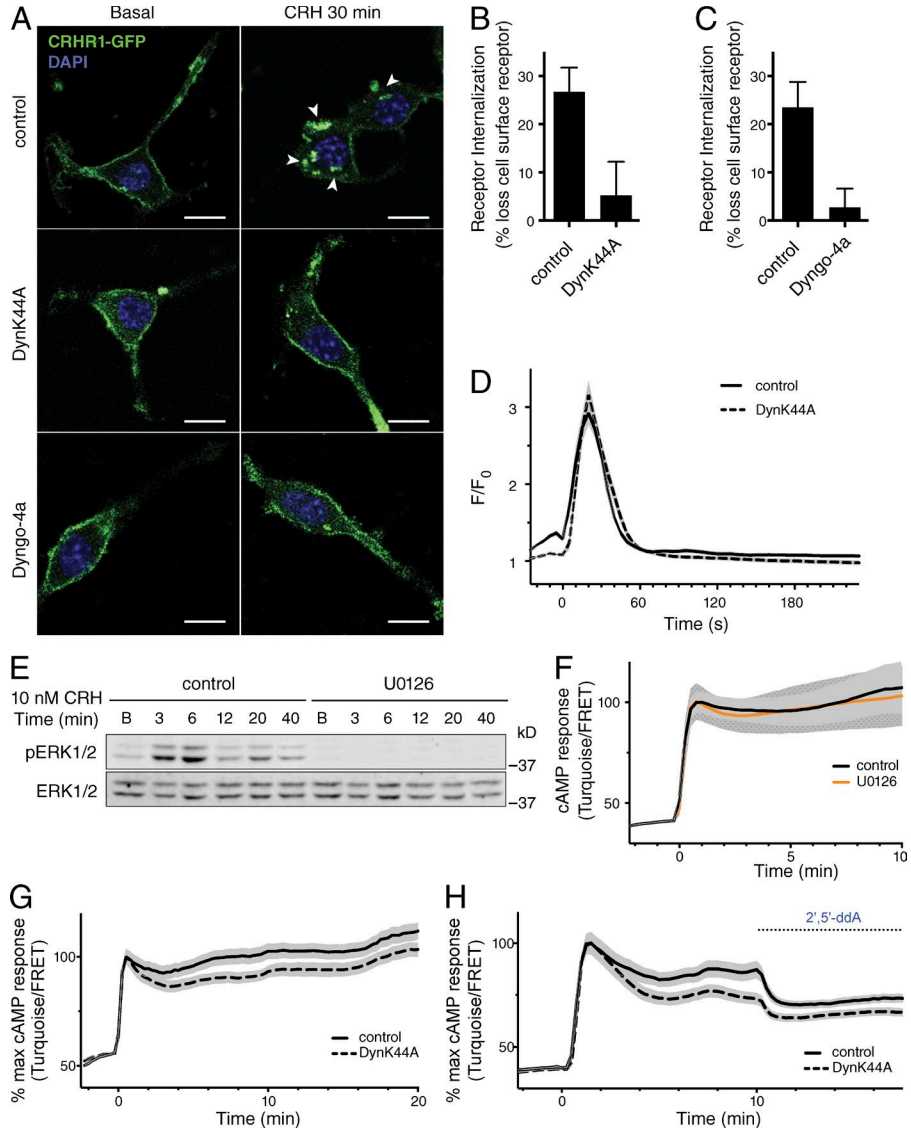

Figure S3. **Endocytosis-dependent response to CRH in HT22-CRHR1 cells.** Effect of endocytosis inhibition by DynK44A or Dyngo-4a was determined by cMyc-GFP-CRHR1 subcellular distribution (A) and fluorescence flow cytometry in HT22-CRHR1 (B and C). (A) Representative fluorescence images obtained of control cells, cells cotransfected with DynK44A, or cells pretreated with 30 μM Dyngo-4a (basal and 30-min 10 nM CRH) are shown. Arrowheads point to abundant internalized GFP clusters after 30 min of CRH treatment in the absence of endocytosis block. Bars, 5 μM. (B and C) Cells were either transfected with pcDNA3 (control) or DynK44A or pretreated with vehicle (control) or 30 μM Dyngo-4a. Surface fluorescence loss after 500 nM CRH for 30 min was determined for each treatment (mean ± SEM, $n = 3$, 10,000 cells/condition, each condition in duplicate). (D) Calcium response was determined in HT22-CRHR1 cells transfected with pcDNA3 or DynK44A, loaded with Fluo-4-AM, and stimulated at time 0 with 100 nM CRH (mean ± SEM, $n = 3$). (E) pERK1/2 and total ERK1/2 were measured in HT22-CRHR1 cells preincubated with vehicle (control) or 10 μM U0126 and stimulated with 10 nM CRH for the indicated times. (F) HT22-CRHR1-Epac-S^{H187} cells preincubated with vehicle (control) or 10 μM U0126 were stimulated at time 0 with 10 nM CRH. Thte time course of FRET changes was measured in single cells (mean ± SEM, $n = 4$). (G and H) Experiment was performed as described in Fig. 6 A. HT22-CRHR1-Epac-S^{H187} cells transfected with pcDNA3 (control) or DynK44A plus mCherry for 48 h were stimulated with 10 nM CRH. (H) When indicated, tmAC-specific inhibitor (100 μM ddA) was added. The time course of FRET changes was measured in single cells.

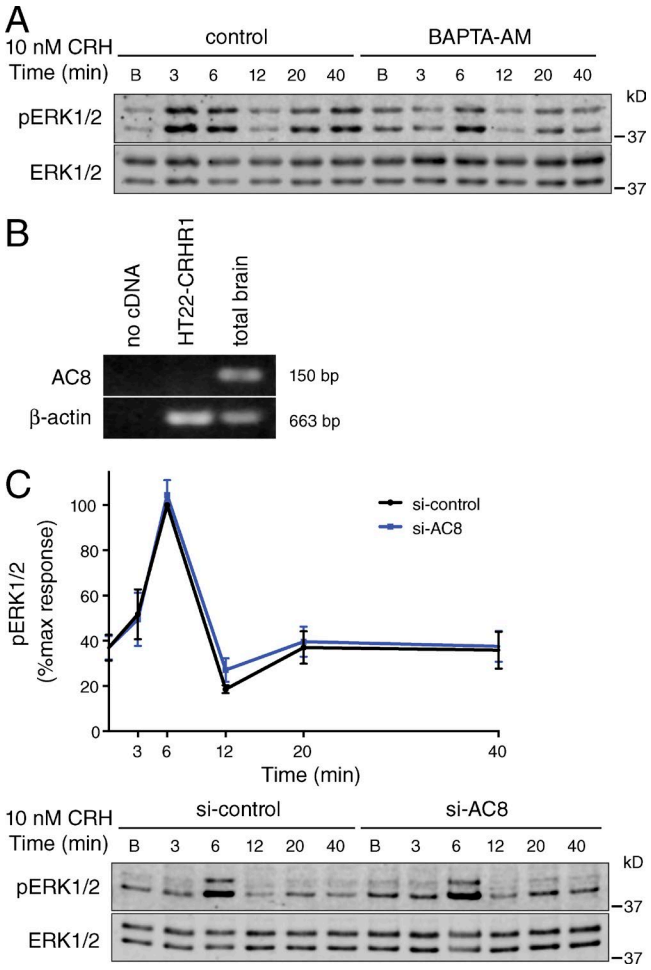

Figure S4. **Calcium regulation of ERK1/2 response triggered by CRH.** (A) pERK1/2 and total ERK1/2 were measured in HT22-CRHR1 cells preincubated in the presence of vehicle (control) or 5 µM BAPTA-AM and stimulated with CRH for the indicated times. (B) AC8 expression was not detected in HT22-CRHR1 cells. AC8 mRNA was amplified by RT-PCR in HT22-CRHR1 cells and total mouse brain extracts (positive control). β-Actin was used as a loading control. (C) pERK1/2 and total ERK1/2 were measured in HT22-CRHR1 cells transfected with 50 nM siRNA against GL3 (control) or AC8 and stimulated with 10 nM CRH. Signals were quantified, and each value of pERK1/2 was normalized to total ERK1/2. Results are expressed as the percentage of maximum pERK1/2 (6 min of CRH stimulation under control conditions). Data: mean ± SEM, $n = 3$. Student's t test was performed for each time point.